Title

Abandoned channel fill sequences in the tidal estuary of a small mountainous, dry-summer river

Journal

Sedimentology, 63(1)

ISSN

0037-0746

Authors

Gray, Andrew B
Pasternack, Gregory B
Watson, Elizabeth B
et al.

Publication Date

2016

DOI

10.1111/sed.12223

Peer reviewed

Abandoned channel fill sequences in the tidal estuary of a small mountainous, dry-summer river

A.B. Gray[a,*], G.B. Pasternack[a], E.B. Watson[a,1], and M.A. Goñi[b]

[a]University of California, Davis, One Shields Avenue, Davis, CA 95616, USA

[b]Oregon State University, 104 CEOAS Administration Bldg., Corvallis, OR 97331-5503, USA

*Corresponding author – Tel.: +1 530-752-1130; E-mail: abgray@ucdavis.edu.

[1]Current affiliation: United States Environmental Protection Agency, Atlantic Ecology Division, Narragansett, RI 02882, USA

ABSTRACT

This study proposes a modification of the current model for abandoned channel fill stratigraphy produced in unidirectional flow river reaches to incorporate seasonal tidal deposition. Evidence supporting this concept came from a study of two consecutive channel abandonment sequences in Ropers Slough of the lower Eel River Estuary in northern California. Aerial photographs showed that Ropers Slough was abandoned around 1943, reoccupied after the 1964 flood, and abandoned again in 1974 with fill continuing to the present. Planform geomorphic characteristics derived from these images were used in conjunction with sub-cm resolution stratigraphic analyses to describe the depositional environment processes and their resultant sedimentary deposits. Both abandonment sequences recorded quasi-annual scale fluvial/tidal deposition couplets. In both cases tidal deposits contained very little sand, and were higher in organic and inorganic carbon content than the sandier fluvially dominated deposits. However, the two abandonment fills differed significantly in terms of the temporal progression of channel narrowing and fluvial sediment deposition characteristics. Aerial photographic analysis showed that the first abandonment sequence led to a more rapid narrowing of Ropers Slough and produced deposits with a positive relationship between grain size/deposit thickness and discharge. The second abandonment resulted in a much slower narrowing of Ropers Slough and generally thinner fluvial deposits with no clear relationship between grain size/deposit thickness and discharge. The $\delta^{13}C$ values and organic nitrogen to organic carbon ratios of deposits from the first phase overlapped with Eel River suspended

sediment characteristics found for low flows (1-5 times mean discharge), while those of the second phase were consistent suspended sediment from higher flows (7-10 times mean discharge). When considered together, the results indicate that the early fill sequence recorded a reach experiencing regular fluvial deposition through flow conditions during the wet season, while the latter fill sequence records a reach more disconnected from the main stem in terms of flow and sediment. The major factor affecting the difference in sedimentation between the two fill periods appears to have been the morphology of the upstream river bend in relation to the position of the bifurcation node and tidal energetics. During the first fill period Ropers Slough seems to have remained open in part due to the placement of its entrance on the outside of the mainstem river bend, and stronger tidal flows caused by a larger tidal prism and close proximity to the tidal inlet. By the second fill sequence the upstream bend morphology had altered, placing the entrance to Roper's Slough on the inner bank of the mainstem bend. Ropers Slough also experienced weaker tidal flows during this period due to a reduction in tidal prism caused by aggradation in the lower Eel Estuary during the 1964 flood, and a more distal tidal inlet due to northerly migration of the Eel River mouth.

INTRODUCTION

Tidally influenced abandoned channel deposits are important as valuable records of autogenic processes and allogenic signatures related to tectonism, climate, sea level fluctuation, salinity, hydrology, and upper basin and in-situ environmental history. Abandoned channel fills of

lowland meandering and anabranching rivers comprise a significant proportion of the terrestrial sedimentary record, yet very few studies have focused on their generation and structure (Toonen *et al.*, 2012). Even fewer studies have addressed the process of channel abandonment and fill in tidally influenced settings, despite the fact that tidal river reaches are spatially contiguous with a large proportion of the human population, and are extremely productive habitats for marine and fluvial organisms (Kleinhans *et al.*, 2010). As such, the hydro-geomorphic and sedimentation dynamics of tidal river reaches are of great importance in terms of human interests such as flood control and navigation, as well as ecosystem services.

The fluvial model

Although Fisk (1947) proposed an initial conceptual model for abandoned channel fill development in a purely fluvial context, only a handful of case studies have examined the stratigraphy of abandoned channels produced under conditions recorded over historic time (e.g. Hooke, 1995; Werritty *et al.*, 2006; Constantine *et al.*, 2010, Toonen *et al.*, 2012). These studies, and that of Shields and Abt (1989) on human constructed fluvial lakes, have shown that the progression of sedimentation in abandoned fluvial channels is the result of internal (autogenic) and external (allogenic) controls on the apportionment of sediment and water to each bifurcate (Kleinhans *et al.*, 2013). The most important autogenic factors include (i) the morphology of the bifurcation zone and (ii) the bed level/downstream channel slope of each bifurcate, which is largely controlled by (iii) bifurcate length, and (iv) bed roughness. The morphology of the bifurcation zone is commonly described by such measures as (a) divergence

angle – the angle between the mean directions of main and abandoned channel flows, or (b) divergence radius, both of which were initially identified by Fisk (1947) and supported by the observational studies above. However, bifurcate morphology can also be strongly influenced by upstream channel meander morphology, with the position and curvature of the nearest upstream channel bend often controlling the curvature and divergence angle of the bifurcation zone. Numerical modeling exercises have confirmed the mechanisms behind the effects of local and upstream channel morphology on abandoned channel sedimentation (Constantine *et al.*, 2010; Kleinhans *et al.*, 2011), in addition to bank strength (Sun *et al.*, 1996), and upstream meander position (Kleinhans *et al.*, 2008). More purely allogenic controls have also been observed, including discharge magnitude/frequency and sediment load characteristics (Citterio & Piégay, 2009; Hoek *et al.*, 2011).

Generic models of abandoned channel fill architecture have evolved over nearly 70 years (Fisk, 1947; Allen 1965; Gagliano and Howard, 1984; Bridge *et al.*, 1986; Shields and Abt, 1989) as recently summarized by Toonen *et al.* (2012). The generic model of fluvial abandoned channel fill sequences describes two end members driven by fluvial sediment connectivity between the major channel and abandoned channel, which is largely controlled by the development of plug bars at the entrances of the abandoned channel (Fig. 1). On one end of the spectrum abandoned channels continue to receive regular throughflow and entrained bedload, while on the other 'oxbow lakes' have both entrances blocked from the main channel during within-bank flows (Allen, 1965). As traditional oxbow lakes are outside of the purview of this study,

comparisons here will focus on the effect of greater or lesser connectivity in terms of hydrology & sediment entrainment between the main and abandoned channels. With greater hydro-sedimentological connectivity, and generally less plug bar formation, the abandoned channel geometry (width, depth) is reduced more rapidly over time. With high bedload connectivity channel fill will be predominantly thick deposits of material similar to the underlying channel bed. Abandoned channels with less regular throughflow connectivity and little or no entrainment of bedload from the main channel tend to fill more slowly, and with much finer sediment that can contain seasonal and event based laminations. Abandoned channel fills commonly progress from greater to lesser mainstem connectivity over time, as plug bars form at the entrance/exit of abandoned channels due to flow separation/backwater effects, and eventually block bedload and suspended load connectivity during in-channel flows (Fisk, 1947). Increased divergence angle, often as a result of local sinuosity, increases the rate of plug bar formation, which decreases the time period of effective bed load advection into the abandoned channel, and more rapidly disconnects it from main channel flows and all classes of fluvial sediments.

New conceptual model

Despite these advances in the understanding of abandoned channel development and alluviation, little has been done to address systems experiencing fluvial and tidal forcings. Most of the studies that established the principles of channel fill dynamics focused on meandering gravel to coarse sand bedded rivers that accomplished meander abandonment through neck or

chute cut-offs, and without reoccupying abandoned channels. These rivers were also driven by strictly fluvial regimes, far upstream from the influence of tides.

Channel abandonment and fill in a tidal river reach is influenced by both fluvial and tidal forcings. The balance of fluvial and tidal forcings determines the relative importance of each in terms of local hydrology, sediment transport dynamics, and geomorphic evolution (van Veen *et al.*, 1950 (republished (2005); Robinson; 1960). With the inclusion of tidal influence, additional factors must be considered in the process of channel abandonment and fill. Tides impose a cyclical modulation of the water surface elevation at the tidal inlet, thus affecting a first order control on downstream boundary conditions (Kleinhans *et al.*, 2010). One indication of the magnitude of tidal forcing is tidal prism -the difference in water volume of a tidal water body at high and low tide. The interaction of tidal prism and the morphology of a river reach, especially bed slope, plays a large role in determining how far upstream tidal effects (salinity, stage modulation) will penetrate. The other major factor controlling the penetration of tidal effects is the magnitude of fluvial discharge relative to the tidal prism. Increasing river discharge magnitude tends to damp out the hydrodynamic effect of tides. Thus the balance of downstream tidal forcings and upstream fluvial forcings interact with each other and the internal characteristics of tidal river reaches to determine the hydrodynamics that exert first order controls on the movement of water and sediment through the system. Given fixed system geometry and upstream boundary conditions, tidal river reaches that are exposed to a larger tidal prism at a shorter distance from the tidal inlet will experience stronger

hydrodynamic effects from tides. Lowering river discharges relative to tidal forcings will result in larger stage modulation proportional to mean stage through backwater effects, and ultimately bi-directional river flow when river inputs are low relative to tidal prism, and the distance to the tidal inlet is short relative to tidal penetration.

Changes in tidal and fluvial magnitudes over time result in temporal patterns of relative tidal and fluvial dominance, which can in turn influence the geomorphic and sedimentary evolution of abandoned channels. Tides generally follow monthly cycles of high (spring) and low (neap) magnitude, and the relative magnitude of spring/neap tides tend to have seasonal scale cycles. Fluvial output also tends to vary cyclically over time, from the event scale (i.e. rising and falling flood discharge), to seasonal (e.g. alternating wet and dry seasons), and interannual to decadal scale cycles such as droughts or periodic large flooding events driven by regional climatic regimes and cycles. Periodic low flow conditions at the seasonal scale are typical of river systems that are small (drainage area < 10^4 km^2), and/or experience a highly variable precipitation regime with inundation cycles at seasonal to inter-annual time scales typical of semi-arid, dry-summer or monsoonal climates (e.g. Puckridge *et al.*, 2000; Andrews *et al.*, 2004).

Thus geomorphic and stratigraphic change in tidal river reaches experiencing strongly seasonal flow is governed by interplay between two distinct and oscillating regimes: tidal and fluvial. During periods of fluvial domination the system would be expected to behave similarly to the

purely fluvial model described above. An important caveat is that tidal backwater effects and the introduction of higher density (saline) ocean waters may impose significant controls despite apparent dominance of fluvial processes. These impacts may include influences on channel bed mobility from salt wedge sheltering, and suspended sediment deposition through (i) salinity induced flocculation and (ii) backwater effects during high tides.

During periods of tidal domination the channelized system would be expected to behave more like tidal channels and sloughs experiencing bi-directional flow. Purely tidal and tidally dominated systems develop channel morphologies consistent with mutually evasive flood and ebb flow (van Veen *et al.*, 2005; Robinson, 1960). Residual sediment transport results from residual net flow due to an imbalance in the ebb and flood velocities found in most tidal channels, with 'flood channels' exhibiting net landward transport of sediment, and 'ebb channels' net seaward transport. Flood channels tend to be deeper to seaward and shallow out at their heads, while ebb channels are shallower to seaward.

The ramifications of this phenomenon in terms of channel abandonment progression include the possibility of the abandoned channel functioning as flood channel counterparts of the axial main/ebb channel (Robinson, 1960; Kleinhans *et al.*, 2013). In this scenario the mutually evasive characteristics of bi-directional tidal flow has potential geomorphic and sedimentary effects that interact with fluvial forcings. Abandoned channels are adjacent to the dominant channel and tend to fill in from their upstream end including the development of plug bars. As

these channels are adjacent to the burgeoning mainstem bifurcate, they would be expected to function as a flood channel, which would further reinforce the pattern of deposition at the upstream end of the abandoned reach, and perhaps act to scour the downstream end of the reach, maintaining the downstream opening.

It is expected that an accreting abandoned channel in an estuary experiencing seasonally oscillating tidal and fluvial domination would produce deposits of alternating tidal and fluvial character. Tidally dominated deposits would be expected during periods of low fluvial discharge, with fluvial deposits produced during high discharge periods (van den Berg *et al.*, 2007). Furthermore, one would expect to find smaller scale tidal sedimentary structures related to spring/neap cyclicity, as well as the possibility of individual flood signatures (van den Berg *et al.*, 2007). Aggrading channel bifurcates with little plug bar formation are expected to act as a high water sub-channel subject to throughflow (with or without bed load transport) during peak winter flows, and then as a flood channels/tidal sloughs fed through the downstream entrance during low discharge periods. Tidal action may also influence the evolution of these systems over periods greater than the time scale of abandonment, as the scouring of tidal flows can maintain the downstream entrance opening (van Veen *et al.*, 2005; Haltiner and Williams, 1987; van den Berg *et al.*, 2007), and prolong a gradient that may increase the likelihood of reoccupation during high flow events (Smith *et al.*, 1998; Stouthamer, 2005). Conversely slight differences in tidal phase between two bifurcates can also favor one branch over the other in terms of flow, and contribute to the process of abandonment

(Kleinhans *et al.*, 2010). Coarser grained, less cohesive fluvial fill can also favor reoccupation by providing a more easily erodible break among more cohesive channel banks materials (Aslan *et al.*, 2005).

The objectives of this study were to: (i) link the stratigraphic characteristics of the fill of a tidally influenced, abandoned river channel in the estuary of a dry summer coastal system to precise periods of geomorphic activity, (ii) determine if the resultant sedimentary characteristics could also serve as indices for historical river discharge magnitude, (iii) identify the mechanisms behind differences in two consecutive sequences of geomorphic change and stratigraphic fill, and (iv) use the insights of this case study to modify the generic through flow and overbank channel fill model for a tidal system experiencing a seasonal fluvial regime. It was expected that the same autogenic and allogenic factors operating in strictly fluvial systems would greatly affect the overall progress of channel filling, namely diversion angle and upstream bend placement effects on bedload entrainment, and that changes in tidal forcing could also exert important controls. The general approach to these issues employed a combination of sedimentary, aerial image and hydrologic analyses.

STUDY REGION

The Eel River drains 9500 km^2 of mostly steep, forested terrain of the north California Coast Ranges to the NNW through a highly episodic hydrologic and sediment transport regime. Regional climate is dry summer temperate with cold wet winters, and dry warm summers. About 90% of precipitation is delivered between October and May. For this reason 'water years' in the region are defined as running from October 1st of the previous year to September 30th of the year in question. A high gradient of precipitation (250 – 50 cm/yr) extends from the coast region to the interior of the watershed. The Eel River over the base period of water years 1911 to 2012 was estimated to have a mean discharge (Q_{mean}) of 230 m^3s^{-1}; a mean peak annual discharge of 5560 m^3s^{-1}, and 10- and 100-year recurrence interval peak mean daily flows (estimated through log Pearson Type III flood frequency analysis) of 10,100 $m^3s^{-1}$and 15,700 m^3s^{-1}, respectively. These estimations were based on USGS records from the lowest gauge in the basin (USGS #11477000, *Eel River at Scotia, CA*), which were increased by 10% to estimate the contribution of flow and sediment from the Van Duzen River, a major tributary of the Eel River that enters below the Scotia gauge, and the small proportion of contributing area below the confluence with the Van Duzen. The Van Duzen generally displays similar hydrologic response timing to the Eel River, and this modification to estimates of Eel River fluvial components is consistent with previous studies (Sommerfield *et al.*, 2007; Warrick, 2014).

This study focused on the vicinity of Ropers Slough, an abandoned channel in the Eel River Estuary, a bar built estuary which lies ~ 7 km south of Humboldt Bay (40°38'21.46"N, 124°16'11.79"W) (Fig. 2). The Eel River Estuary is the fourth largest in California, with an

inundated surface area of ~ 24 km^2 at high water, and is generally defined as the network of lower Eel River channels and tidal sloughs, and intertidal and overflow lands downstream of the town of Fernbridge, California (CDFG, 2010; Schlosser & Eicher, 2012). Gross stream gradient of the estuary from the Eel River mouth to Fernbridge, CA is ~ 0.0003. Reaches in the study area were defined on the basis of bifurcation and convergence nodes in the lower Eel Estuary (Fig. 2). A major bifurcation (Node 1) splits the lower Eel River Estuary channel into two bifurcates defined as (i) the South Channel and (ii) the Ropers Slough/Central Channel Complex (RSC). The RSC was further subdivided due to a secondary bifurcation (Node 2) into Ropers Slough and the Central Channel. Downstream convergence nodes are defined as the confluence of Ropers Slough and the Central Channel (Node 3) and the confluence of the RSC and the South Channel (Node 4). The distance from Node 3 to the mouth of the Eel River has varied from ~ 3 – 6 km between 1955 and 2009, primarily due to the migration of the mouth of the Eel River. Current mean bankfull depths of Ropers Slough and the Central Channel are on the order of 2 and 4 meters respectively. Ropers Slough has existed at times as the major channel in the RSC complex, and at others as an abandoned high water channel/tidal slough, the details of which will be explored more fully in the following sections.

Early reports from settlers in the 19th Century indicated that the Eel River Estuary was largely forested with pine, spruce, alder and redwoods, almost all of which was cleared by the late 1800s (Schlosser & Eicher, 2012). Today tidal mudflats and marshland mostly exist along main and recently abandoned fluvial channels in the central portion of the estuary, and along the

northern tidal slough complexes. Vegetation assemblages in the brackish tidal marshes on the margins of Ropers Slough are dominated by C_3 vegetation including seacoast bulrush (*Bolboschoenus maritimus* L.) and Lyngbye's sedge (*Carex lyngbyei*) (Schosser & Eicher, 2012; personal observations of the authors). Plants using the C_3 pathway carbon fixation remove carbon directly from the air rather than through a malate intermediary, as in C_4 plants, which results in differences in $\delta^{13}C$ in organic matter produced through these two pathways. Average vegetation throughout the upper Eel River watershed includes a mix of C_3 and C_4 plants.

Tides at the Eel River Mouth are mixed semi-diurnal with a mean range of 1.34 meters, and mean annual lowest and highest tides of -0.52 m and 2.31 m, respectively (Eel River Entrance California Tide Chart: http://www.tide-forecast.com/locations/Eel-River-entrance-California). Tidal influence in terms of salinity currently extends about 11 river km upstream to the town of Fernbridge (USGS gauge #11479560 Eel R at Fernbridge, CA, elevation: 1.2 m), where salinities of 2 – 11 ppt have been measured, but only during the periods of lowest river flows in the dry season ($Q < 7\ m^3s^{-1}$) (Boles *et al.*, 1977; Cannata and Hassler, 1995). Earlier in the 20th Century salinity influences extended as far as 16 km upstream (Schlosser & Eicher, 2012). Tidal backwater effects on river stage regularly extend 11 km upstream to Fernbridge during low river flows. Tidal modulation at Fernbridge results in maximum stage increases of ~ 0.6 meters at high tide during the summer dry season resulting in slower flow velocities, but not flow reversal at this location. High tide stage lag from the Eel River mouth to Fernbridge is approximately 1 hour (CDFG, 2010). Tidal stage modulations were observed as far as 23 km

upstream from the Eel River mouth to the confluence with the Van Duzen River earlier in the 20th Century (elevation: 10 m) (Boles *et al.*, 1977; Van Kirk, 1996).

The decreases observed in both salinity intrusion and the penetration of backwater effects are attributed to reduction of the Eel River Estuary tidal prism due to channel aggradation and land reclamation since the mid-19th Century (SCS 1989; Schlosser & Eicher, 2012). Tidal prism was most likely decreasing by the early 20th century, and is estimated to have experienced a ~ 40% decreased since 1900 (SCS, 1989). Much of this reduction is attributed to increasing sediment loads in the middle of the 20th Century, driven in part by large floods, including a ~ 200 year event (peak discharge > 20,000 m^3s^{-1}) that occurred in December of 1964, and drastically filled the deeper pools of the south channel (Haley, 1970; Boles et al., 1977; Puckett, 1977; Li *et al.*, 1992; Van Kirk, 1996). In fact, these rare high discharge events on the Eel have produced larger sediment yields than perhaps any other river in the U.S. (Brown & Ritter, 1971; Kelsey, 1980; Warrick *et al.*, 2013; USGS NWIS, 2014). The high sediment load of the Eel River is driven by large storm events acting upon extremely erodible geology, especially the mass wasting prone Franciscan mélange, a highly deformed class of Cenozoic metasedimentary marine rock that underlies the central portion of the basin (Kelsey, 1980, McLaughlin *et al.*, 1989). High sediment loads appear to have been further exacerbated by large scale industrial timber harvesting, which began in the late 19th Century and continues to be the largest human impact in the watershed (Kelsey, 1980; Warrick *et al.*, 2013). The latest studies on suspended sediment dynamics of the Eel River and neighboring systems have shown that the 1964 flood engendered

a period of increased suspended sediment load that has relaxed over the latter half of the 20th and beginning of the 21st Centuries (Madej *et al.*, 2012; Warrick *et al.*, 2013; Warrick, 2014).

Previous geomorphic and sedimentological work in the Eel Estuary documented the channel aggradation/avulsion history in the vicinity of Ropers Slough, and estuarine scale sedimentation. Haley (1970) described the major morphological changes in the Eel River Estuary between 1950 and 1969, including the aggradation of deep pools in the south channel after the 1964 flood. Puckett (1977) documented subsequent changes to the Eel Estuary channels through the initiation of the second abandonment of Ropers Slough in 1974. Boles *et al.* (1977) characterized channel bed sediment in terms of texture classes on the basis of samples collected from 1975 – 1976. Li *et al.* (1991) collected three sediment cores from the Eel Estuary and posited that late Holocene deposition at the estuarine scale was controlled by infrequent episodes of rapid subsidence. A recent report by Schlosser and Eicher (2012) characterized changes in Eel River Estuary benthic habitat types from 1948 to 2009 on the basis of high resolution aerial imagery and ground surveys.

MATERIALS AND METHODS

This study was based on environmental measurements and interpretations collected from aerial photographs, and high resolution sedimentological analyses on records from a single

coring location in the upstream reaches of Ropers Slough. The time series of aerial photographs provided a record of planform geomorphic change across the entirety of the RSC complex.

Planform geomorphology

The planform evolution of Eel River channel structure in the vicinity of Ropers Slough was reconstructed from 20 aerial photographs collected between 1940 and 2009, and obtained from the USGS (USGS Earth Explorer, 2014) (Table 1). This photo sequence includes two cycles of Ropers slough channel abandonment (Fig. 3). Channel abandonment times were assigned to the date of highest daily discharge at the Scotia gage between the date of the most recent photographs before and after abandonment. Photographs without spatial references were georectified in ArcGIS 10.1 with a 3rd degree polynomial transformation using 11 to 30 georeferenced control points tied to 0.5-m resolution orthorectified photographs collected in 2009 for the Humboldt Bay and Eel River Estuary Benthic Habitat Project (Hughes *et al.*, 2006; Schlosser & Eicher, 2012). Median spatial resolution (raster cell size, *R*) for the entire time series of photographs was 2.24 m with a range of 0.50 to 8.16 m. The median RMSE of referencing errors (spatial distortion, *o*) was 0.85 m with a range of 0.08 to 4.7 m.

Serial photographs documenting 20 dates from 12/13/1940 to 7/27/2009 were used to compile the following time series: (i) the depositional/erosional environment at the sediment core

collection site, (ii) the location of the upstream entrance to Ropers Slough relative to the meander morphology of the RSC complex, and (iii) measurements of channel characteristics. The geomorphic setting of the core location was determined for each photo as (i) major fluvial through-flow channel bed, (ii) minor fluvial channel/tidal slough channel bed, or (iii) emergent marsh. Assigned geomorphic setting was highly certain, as the core location was sufficiently far from geomorphic boundaries for each time period to be unaffected by the combination of spatial error ranges. The entrance of Ropers Slough was identified as located either on the outer bank or inner bank of meander bends in the RSC complex.

Three channel characteristics (cutoff ratio, diversion angle, and average active channel width) were measured for each reach using ArcGIS 10.1. For channel cutoff events, the cutoff ratio is the length of the abandoned channel divided by the length of the cutoff channel. To calculate cutoff ratio, channel lengths were measured in ArcGIS 10.1 along the estimated thalweg between characteristic nodes. Diversion angle is the angle between average flow direction in the cutoff channel and flow into the entrance of the abandoned channel (Fisk, 1947). Diversion angle was calculated from the vertices of main channel and sub-channel centerlines measured from the earliest photograph after the cut-off. Active channel width was defined as the distance between vegetated banks normal to the channel centerline. It was measured in 20 equally spaced increments for each reach. Planimetric measurement errors (ε_m) were assumed to be isotropic and thus calculated as per Mount *et al.* (2003).

Sedimentology

A single stratigraphic record was collected on 7/23/2008 from a middle-zone, brackish, tidal marsh surface located on the interior portion of Ropers Slough (hereafter referred to as the single coring location from the Eel Delta in Ropers Slough, 'EDRS'), (Figs. 2, 3). Although a single coring location cannot provide the sedimentological counterpart to the geographic extent of the planform record, EDRS was well situated to record a sedimentary signature of reach-scale hydro-geomorphic events. The upstream portion of Ropers Slough experienced fill during two successive periods of channel abandonment – retrieval of a core from this reach increased the likelihood of capturing tidal and fluvial deposits. Although core location appeared to be near the outer bend bank during the first abandonment sequence, the thalweg was clearly compressed to this area through rapid channel fill extending from the inner bend. During core collection EDRS was observed to be more than 20 meters away from the relic eastern bank of Ropers Slough. Thus, it was deemed likely that EDRS recorded general fill characteristics of the upper reach, rather than localized issues such as bank slumping.

The site was vegetated primarily with *Carex lyngbyei*. To avoid problems caused by coring through a vegetated mat, the record was obtained using a pair of sediment cores of overlapping depth- one including the vegetation (0–38 cm depth) and one obtained 50 cm laterally from the first starting below the vegetation (21.5 to 303 cm depth). The short section was hammer driven, while the long section was recovered using the vibracoring method with a piston to generate suction up the tube. Cores were transported to the laboratory, split,

photographed, and described. Archival acrylic D-channels were digital x-radiographed at the University of California at Davis Veterinary Medical Teaching Hospital. Sediment horizons were sub sampled on the basis of stratigraphic intervals for particle size distribution, inorganic and organic carbon content, stable carbon isotopes and ^{14}C radiometric dating.

Particle size distribution analyses were run on 195 horizons. Sediments with diameters less than gravel (diameter (D) < 2000 µm), were processed for particle size distribution analysis using a Beckman Coulter LS-230 as per as per Gray *et al.* (2010). The gravel fractions of coarse horizons were characterized by nested ½ ϕ intervals. Additional particle size distribution data for channel bed, bed load and suspended sediment samples collected by the USGS from the *Eel River at Scotia, CA* gaging station (#11477000) were processed by the USGS using mass based sieving and settling techniques (USGS NWIS, 2014). Log-linear rating curves of suspended sediment concentration (C_{SS} (mg L^{-1})) vs. water discharge (Q, (m^3s^{-1})) were also plotted for each ϕ interval and texture class. All particle size distribution data were analyzed with GRADISTAT v.8 to compute descriptive statistics in units of µm and ϕ based on the logarithmic method of moments (Folk, 1974; Tanner, 1995; Blott & Pye, 2001,). Sediment texture classes (e.g. clay, silt, sand, etc.) were reported as per the Blott and Pye (2001) modified Udden/Wentworth scale (Wentworth 1922), with the exception that the original clay/silt transition of 4 µm was maintained.

Carbon and nitrogen content measurements were performed on homogenized bulk sediment samples using established techniques reported elsewhere (Goñi et al., 2006; 2013). Bulk analyses results included weight percent total carbon (%TC), organic carbon (%OC) and organic nitrogen (%ON), molar carbon to nitrogen ratios (OC:ON), inorganic carbon (%IC), and stable isotopic compositions of organic carbon ($\delta^{13}C$). Replicate analyses of selected samples for percent compositions yielded analytical variability of less than 4% of the measured values, and analytical reproducibility of $\delta^{13}C$ measurements was better than 0.3 ‰.

Post-bomb ^{14}C measurements and calibration was used to establish absolute horizon dates. Post-bomb radiocarbon techniques exploit the fact that above ground nuclear explosions in the 1950s and 1960s caused a rapid increase in atmospheric ^{14}C levels, which have been declining since the mid-1960s due primarily to mixing of global CO_2 reservoirs (Rafter & Fergusson, 1957; Buchholtz, 2009). The short period of deposition examined here required further care in sample selection to minimize the time lag between biological material generation and horizon deposition. Thus radiocarbon sample selection from EDRS horizons was constrained to autochthonous *Carex* and *Bolboschoenus* seeds and leaves, and intact, green sections of *Elodea canadensis*. *Elodea* does not occur as rooted stands in the brackish waters of Ropers Slough but is present in the lower Eel River mainstem only several kilometers up stream, and seasonally shed sections are carried downstream by river flow. Five samples obtained from four horizons were cleaned and processed for accelerator mass spectrometry (AMS) measurements of fraction modern ^{14}C ($F^{14}C$) and $\delta^{13}C$ using the standard acid/alkali/acid procedure followed by

graphitization at the National Ocean Sciences Accelerator Mass Spectrometry Facility (NOSAMS) and the Lawrence Livermore National Laboratory Center for Accelerator Mass Spectrometry (CAMS). Estimations of $F^{14}C$ were calculated as per Reimer *et al.* (2004) with corrections for $\delta^{13}C$ and background interference. In cases where $\delta^{13}C$ was not measured at the AMS facility due to small sample size, the average $\delta^{13}C$ obtained through mass spectrometry of 56 EDRS horizons was used to revise $F^{14}C$. The $F^{14}C$ error in these cases was also revised based on $\delta^{13}C$ measurement error and the standard deviation of EDRS horizon $\delta^{13}C$ values combined in quadrature. Date ranges for $F^{14}C$ values were calibrated using the CaliBomb program set to NH Zone 2 (Reimer *et al.*, 2013). Although EDRS is located near the border of NH Zones 1 and 2, the differences in calibrated dates were on the order of < 1 year, and insignificant for the purposes of this study.

DATA ANALYSIS

A general stratigraphic zonation of the EDRS core was developed on the basis of sediment texture and layering. Basic horizon types were defined by particle size distribution characteristics. Facies units were then composed of adjacent similar horizons. This lithostratigraphy was then set within the chronostratigraphic model and accompanied by carbon composition results. The chronostratigraphic model was based on a combination of bomb calibrated ^{14}C dates in the context of the geomorphic conditions interpreted from aerial photographs, the Eel River hydrograph and stratigraphic changes. Comparisons of particle size

distribution descriptors between populations of samples were achieved through mean state comparisons using T-tests (threshold of significance $p \leq 0.05$) with the conservative assumption of unequal variance (Helsel & Hirsch, 2002). Particle size distribution characteristics were then plotted in statistical domains developed by Tanner to further evaluate shifts in transport agency and depositional regimes (Tanner, 1991; Larrio *et al.*, 2002; Watson *et al.*, 2013).

RESULTS

Depositional environments

The two channel abandonment cycles of Ropers Slough resulted in three depositional environments at EDRS over the period of accretion: (i) major fluvial channel, (ii) abandoned channel with seasonal throughflow, and (iii) tidal slough/marginal emergent marsh (Table 2). It was assumed that the first abandonment, which occurred between the 1940 and 1948 photographs, took place during the highest magnitude event of that time range (8920 m^3s^{-1}, 1/21/1943). The 1943 discharge event was 2000 m^3s^{-1} greater than any other event during this time period. Channel avulsion/reoccupations generally occur during high discharge events in low gradient rivers (Hook, 1995; Constantine *et al.,* 2010), as chute cutoffs require high water levels and high bedload transport rates of large floods to initiate erosion of the new channel, and aggrade the abandoned channel, respectively (Lewis and Lewin, 1983; Howard, 1996; Ghinassi, 2011; Zinger et al., 2011). High flow events were also found to cause other

abandonment scenarios on the Eel River while reviewing aerial photographs, including the second Ropers Slough abandonment, which was photo documented during the 8000 m^3s^{-1} event of 1974.

Channel geometry

Diversion angle, the basic geometric relationship between the post abandonment main channel flow direction and channel inlet flow direction, was identical for the two abandonments at 66.2 and 67.3 ± 3°, respectively (Table 2). Cut-off ratios were also equivalent. However, progression of subsequent channel narrowing was very different, with Ropers Slough narrowing much more rapidly after the 1943 abandonment than after 1974 (Fig. 4,5). Geomorphic differences between the two eras of Ropers Slough abandonment included the placement of the entrance of the RSC complex (Node 1), and the Ropers Slough channel entrance (Node 2) relative to upstream meander bend morphology (Table 2, see Figs. 3,4).

These observations indicate that the partitioning of water and sediment supply to Ropers Slough and the Central Channel after each cutoff event may have been controlled in part by the location of the entrance to Ropers Slough relative to the meander morphology of the RSC complex. It has been shown that helical flow patterns from upstream channel curvature can result in the delivery of more channel to one bifurcate, and more sediment to the other (Kleinhans *et al.*, 2011; van Dijk *et al.*, 2014). During the 1943 to ~ 1965 abandonment

sequence the entrance of Ropers Slough was located on the outside of a northeast facing meander bend in the RSC complex (Table 2, see Figs. 3,4). During the second abandonment sequence from 1974 to the present (2014), the entrance to Ropers Slough was located on the inside of a very low sinuosity bend of the RSC complex. Furthermore, the entrance of Ropers slough itself in this case was a bend of the RSC complex that was actively accreting a point bar before abandonment. This point bar occupied the same location as the subsequent plug bar that continued to accrete across the entrance of Ropers Slough after abandonment.

Chronostratigraphic model

Post-bomb radiocarbon dating revealed that EDRS was accreted over the last half of the 20th to early 21st Centuries (Table 3, Fig. 4). As this time period traverses the rise and fall of the bomb derived ^{14}C spike in the atmosphere, and as such produces two age ranges for each $F^{14}C$ value, directional evolution of the sedimentary sequence is used to guide age range selection. Sediment superposition and photographic evidence of the timing of geomorphic change at the site, particularly the fact that the site was located in the main RSC channel complex from at least 1965 through 1974, allowed for a confident choice of age ranges for the resultant stratigraphic model.

Stratigraphic zones

Four general stratigraphic zones were defined on the basis of sediment texture and the presence of plant macrofossils (Fig. 4). The major textural dichotomy found in EDRS was the presence of horizons composed entirely of fines versus those containing sand.

Zone 1, which extends from the surface to a depth of 164 cm is composed of a series of two alternating characteristic units (i) distinct sandy silt horizons lacking internal structure and ranging from 0.5 to 5 cm thick, and (ii) finely laminated (mm scale) clayey silts of ~ 1 to 40 cm thickness, which occasionally contain sandy laminations (Fig. 4). No trends in the particle size distribution metrics D_{10}, D_{50} and D_{90} were found for Zone 1 with depth. Both unit types contained abundant plant macrofossils to a depth of about 1 m, and were penetrated by roots to a depth of 140 cm, becoming less abundant down core.

Zone 2 extends from 164 to 195 cm and is composed entirely of sandy silts, and sands (Fig. 4). Unlike the unstructured coarse layers of Zone 1, Zone 2 sandy silts also appeared to have mm scale laminations. Sand dominated layers display wavy bedding structures, apart from the lowest unit, which contain sand supported clay clasts. Examination of horizon D_{50} values showed that the overall Zone 2 particle size depth trend is that of a fining up sequence. Coarse fraction trends as indicated by D_{90} were stable with the exception of the lowest, coarsest, clay-clast bearing zone. Plant macrofossils and roots are notably sparse in Zone 2.

Zone 3, extending from depths of 195 to 221.5 cm is characterized by a 20 cm thick gravely sand unit (depth 201 to 221 cm) bound above and below by thin layers of silty sand, the upper of which fines up into an unstructured layer of clayey silt (Fig 4). The upper silt layer was the only found to contain plant macrofossils. Gravel sizes display a double peak with depth, the coarser of which (depth range 205 to 209 cm, D_{90} =9045.6 μm) coincides with the highest proportion of gravel. Very little organic material was present in Zone 3.

Zone 4 (depth 221.5 to 303 cm, end of core) is composed of three unstructured sandy horizons (two dominated by sand, one dominated by silt) alternating with mm scale laminated silty clay units (Fig. 4). The two sand dominated horizons (depth ranges 227 to 235 cm, and 245 to 301 cm) are coarser than those found in Zones 1 and 2 above, with D_{90} ranging from 149.5 to 270.5 μm. The relative coarseness of the sandy silt horizon (depth 238 to 243 cm) is similar to those up-core (D_{90} of ~ 100 μm), and was horizontally laminated. This silty sand unit is overlain by a fining-up sequence of clayey silts (depth 235 to 238) capped by a silty clay with the highest clay content found in the core (62.2 % clay). The lowest and coarsest unit was a massive sand body extending from 245 to 301 cm, bound below by a rooted horizon of organic rich silt. The silt layer capping this large sand body is another fining-up sequence topped by the second highest clay content found in the core (33.7 % clay). Plant macrofossils found in Zone 4 were limited to the units of laminar fines.

Geomorphic and stratigraphic reconstruction and synthesis

The sediments sampled by the EDRS cores were deposited beginning on or within a few years of 1957, and ending in 2008. The major features of this deposit (from the bottom up) were: (i) the last years of an abandoned channel fill sequence (Zone 4), (ii) an interval as the main northern channel (RSC complex) (Zone 3), and (iii) a second sequence of abandonment and fill (Zones 2 and 1). The upper contact of the first abandoned fill sequence (Zone 3/4 transition) is most likely an unconformity, as the newly forged RSC complex must have scoured through the top layers of sediment. The differences in inundation between the reach of Ropers Slough that was reoccupied as main channel and that which remained abandoned in 1965 clearly showed that scouring must have taken place. The reorganization of the RSC complex most likely occurred during the large December 1964 flood. Significant geomorphic changes occurred during that event and the new RSC complex was still very narrow in the summer of 1965. Over subsequent years the RSC complex widened and reorganized further by routing through the rest of Ropers Slough and abandoning the Central Channel by 1972.

Although the exact dating of the channel bed deposits in Zone 3 was unclear, a simple interpretation would identify these coarsest of deposits as the product of the largest discharge event, namely the December 1964 flood. However, geomorphic change in the Eel Estuary suggests that this was not the case. The dilation of the RSC complex between 1965 and 1972 was in part the result of the shoaling of the main South Channel by the December 1964 flood. Successive high discharge events did not change this trend, but rather established the northern channel (the RSC complex) as the main channel, scouring it to accommodate greater flow. It is

highly unlikely that a channel would increase in width and discharge capacity to this degree without increasing in depth to some extent. Furthermore, Boles *et al.* (1977) found that the Ropers Slough channel bed surface in 1975 – 1976 was composed of a mixture of fines, sand, and fine gravel. Thus, the coarse deposit in Zone 3 is more likely related to the 1974 flood, which had a peak discharge of 10,959 m^3s^{-1} at Scotia, and an estimated peak discharge to the estuary of ~ 12,000 m^3s^{-1}, and was the third largest discharge of the hydrologic record. Zone 2 then recorded the transition from major to abandoned channel that occurred between ~ 1977 and 1986.

Particle size distribution characteristics of stratigraphic zones

Of the 46 measured fine horizons, 37 were present in Zone 1, and 9 in Zone 4 (Table 2). Fine horizons were poorly sorted, mesokurtic, and fine skewed, displaying single or bimodal peaks in the medium to very coarse silt range (11 to 38 µm) and a characteristic clay shoulder around 2 – 4 µm (Table 2, Fig. 5). Clay/Silt ratios were generally 1:3. Comparison between fine horizon descriptors revealed that only skewness and kurtosis differed significantly between Zones 1 and 4 (slightly higher in Zone 1) (Table 3).

Sandy horizons displayed a greater range of particle size distribution characteristics than fine horizons (Table 3, Fig. 5). In general, sandy horizons were very poorly sorted, mesokurtic to very leptokurtic, fine skewed, and unimodal, with a small proportion of bimodal and poly-modal

horizons found mostly in Zones 3 and 4. Primary modes in Zones 1, 2 and 4 were generally in the coarse silt to very fine sand range (31 to 125 μm). The few secondary modalities in these zones were generally finer, plotting in the coarse to very coarse silt range. In contrast, the majority of Zone 3 horizons were fine skewed, meso to leptokurtic, and bimodal or poly-modal mixes of sand and gravel. Zone 3 primary modes ranged from fine to medium sand (125 to 500 μm), while secondary modes were generally coarser, plotting in the very coarse sand to medium gravel range ($1{\cdot}10^3$ to $1.6{\cdot}10^5$ μm). High variability in texture class composition also belied the range of sediments represented by this group, as horizons varied between clayey silts, with trace amounts of sand, to sand and gravel mixes with very low (<10%) fines (Fig. 5).

Differences in the population means of sandy horizon particle size distribution characteristics between zones ranged from equivalence in nearly every characteristic to significant differences for all characteristics (Table 3). By this array of tests, Zone 2 and Zone 4 sandy horizons were most similar, with equivalence of every characteristic except for % clay. The Zone pairs 1 vs. 4 and 2 vs. 3 each showed equivalence in three metrics, while pairs 1 vs. 3 and 3 vs. 4 were only equivalent in terms of skewness.

Facies Units

Horizons were aggregated into facies units, defined as contiguous horizons with specific grain characteristics. First, horizon types were refined, as highly variable sandy horizon particle size

characteristics within and between zones suggested that further delimitation was necessary. A histogram of sandy horizons by % coarse revealed that three disparate populations of sandy samples were likely: samples with trace (< 7%), moderate (7 to 50 %) and high (> 50%) coarse content with and without gravel (Fig. 6). All sandy populations significantly differed from each other in terms of all mean particle sized distribution descriptors, with the exception of some comparisons to samples with gravel, which were obscured by the high variance of most particle size distribution metrics for these samples (Table 3). Thus, horizons were grouped into four characteristic facies unit types: (i) Fine (0 to 7 % sand), (ii) Medium (7 to 50 % sand), (iii) Coarse (> 50% sand, no gravel), and (iv) Very Coarse (gravelly sand) and were numbered down core by zone (Fig 7).

Carbon composition

Down core variations in organic and inorganic (carbonate) content were informative in terms of marsh development and also provided supporting evidence for tidal vs. fluvial sedimentation regimes. Organic carbon and nitrogen contents were highest near the surface, where roots and large plant debris were most abundant, with additional variability that appeared to be associated with horizon or facies unit type (Fig. 7). High variability of inorganic carbon content and the organic carbon-organic nitrogen ratio also appeared to be closely linked with differences at the horizon or unit level, while horizon type and ^{13}C levels appeared to be unrelated (Fig. 7).

Comparison of Fine and Sandy horizon carbon characteristics between stratigraphic zones revealed more similarities between sandy horizons than fine horizons (Tables 4,5). Fine horizons in Zones 1 and 4 significantly differed in all carbon metrics except for $\%CaCO_3$. Sandy horizons in Zone 1 differed significantly in all carbon characteristics to the Sandy horizons in all other zones except for $\delta^{13}C$ in Zones 3 and 4, and $\%CaCO_3$ in Zone 4. Zone 2 Sandy horizons were generally equivalent in terms of carbon characteristics to those of Zones 3 and 4, with the exception of %OC and %ON of Zone 3 horizons, and $\%CaCO_3$ of Zone 4. Zones 3 and 4 Sandy horizons significantly differed in terms of %OC, $\%CaCO_3$ and %ON.

Systematic inquiry into the relationship between facies units and carbon characteristics showed that organic carbon, organic nitrogen and inorganic carbon contents, as well as OC:ON all significantly decreased with increasing unit coarseness (Tables 4,5). The difference in mean values between each facies unit type were found to be statistically significant in all cases except for Coarse and Very Coarse $\%CaCO_3$ and OC:ON (Tables 4,5). The only significant differences between facies units in terms of $\delta^{13}C$ were between Very Coarse (the most $\delta^{13}C$ enriched) and Fine /Medium units (the most $\delta^{13}C$ poor).

Eel River suspended, bed, and bedload sediment characteristics

Eel River suspended sediment particle size distributions were generally very poorly sorted, symmetrical, platykurtic, and bi- or poly-modal, with nearly equal proportions of clay, silt and

sand (Table 8, Fig. 10). None of the 180 suspended sediment samples contained particles coarser than 2000 µm (very coarse sand). Bed sediment samples displayed a range of modalities and were generally poorly sorted, fine skewed, leptokurtic and composed mostly of equal parts sand and gravel, with only a trace amount of fines (< 2%). Bedload sediment also displayed a range of modalities and was generally poorly sorted, fine skewed, very leptokurtic and composed of primarily sand and gravel. Although no data was presented on fines, the 0 to 250 µm particle size bin averaged ~3% of total sample mass, thus the upper limit of fine contribution to bedload was similar to the fine content of the bed.

Concentration-discharge log-linear rating curves revealed that Eel River suspended sediment particle size distribution was relatively insensitive to discharge, with some notable exceptions (Fig. 11). At $Q \approx 200\ m^3s^{-1}$ silt supplants clay as the primary textural constituent (Fig. 11a) and very fine sand (63 to 125 µm) supersedes fine sand (125 to 250 µm) (Fig. 11b). At $Q > 2000\ m^3s^{-1}$ silt concentrations ≈ 2x clay concentrations, and fine sand concentrations are ≈ 2x very fine sand concentrations. Results of tests for differences in mean particle size distribution characteristics on the following sample populations: (i) $Q < 200\ m^3s^{-1}$, (ii) $200<Q<2000\ m^3s^{-1}$, and (iii) $Q>2000\ m^3s^{-1}$, indicated that these populations were indeed distinct in terms of particle size distribution (Table 9).

Tanner domains: EDRS and Eel River sediment suite statistics

The EDRS horizons and Eel river sediments (suspended, bed and bedload) were compared by plotting suite particle size distribution values in bivariate statistical spaces (Fig. 12). EDRS and suspended sediment sub-populations were further defined by stratigraphic unit and discharge range, respectively. The suite mean vs. sorting space has been commonly used to discriminate between fluvial through-flow channel deposition and settling environments (Tanner, 1991; 1995; Lario *et al.*, 2002; Watson *et al.* 2013) (Fig. 12a). With increasing mean particle sizes (decreasing ϕ), sorting increased in a generally linear fashion for fine through coarse EDRS units and suspended sediment. Increasing mean particle size through the very coarse unit to bedload and bed sediment size range resulted in decreasing sorting values. Fine units and low discharge suspended sediment plotted in the 'closed basin' domain, while medium/coarse units and medium/high discharge suspended sediment samples plotted in the 'fluvial' domain, as defined by Tanner (1991) and refined by Lario et al. (2002). Samples segregated into distinct regions of skewness vs. kurtosis space, one of which was occupied by suspended sediment, another by fine through coarse units, and a third region with very coarse units, bed and bedload samples (Fig. 12b).

The depositional domains defined for this space did not correspond well with thd lower Eel system, as none of these fluvially derived samples plotted near the pre-established fluvial zone. In contrast, all samples plotted into the pre-defined fluvial zone in sorting vs. skewness space, with EDRS units, bed and bedload samples occupying a narrow, fine skewed range, and suspended sediment samples plotting below in the symmetrical to coarse skewed range (Fig

12c). Standard deviation of means vs. standard deviation of sorting space has been used to infer increasing stream gradients as both values increase (Fig. 12d). Indeed, this pattern holds up if very coarse EDRS units are compared to Eel River bed sediments, which were collected from a somewhat steeper reach upstream. Coarsening unit progression followed a linear-like increase in both parameters from fine through coarse units, whereas the progress from low to high discharge samples led to a decrease in the standard deviation of means and sorting.

Hydrostratigraphy

If the ^{14}C based chronostratigraphic model is slightly modified with regard to the time series of discharge events and stratigraphic characteristics to assign time periods of deposition to the abandoned channel fill sequences of Zones 1 and 4, the possibility of stratigraphic characteristic dependence on discharge magnitude can be examined. Here the Zone 1 depositional period was estimated as 1987 – 2008, based on the age of material deposited at depths of 62.5 and 166.5 cm. The 2σ date range for material at 166.5 was 1983.0 to 1986.2. The base of this uppermost unit of Zone 2 was assigned a depositional date of 1986. Further supporting evidence for this date choice were (i) the unit was coarser and thicker than surrounding units and (ii) the 1986 water year produced a maximum Q_d of 8600 m^3s^{-1}, which was 2000 m^3s^{-1} higher than any water year within +/- 9 years. The Zone 4 depositional period was estimated as 1960 to 1964. Two ^{14}C samples collected near the bottom of the core (depths of 302 cm) dated to 1957. The lowest Coarse unit of Zone 4 was the thickest found in the entire core and was

assigned to 1960 because the maximum Q_d of 7400 m^3s^{-1} was ~ 1400 m^3s^{-1} greater than the year with the second highest Q_d (1963) and at least 2500 m^3s^{-1} greater than those of 1957-1959.

Under this modified chronostratigraphy, the Stratigraphic unit and wet season periodicity were found to be very similar in Zones 1 and 4, with 19 couplets deposited over 22 years in Zone1, and 4 couplets deposited over 5 years in Zone 2 (Fig. 13). Departure from a strictly annual resolution may have been related to threshold discharge. A discharge event threshold near 3000 m^3s^{-1} would result in the same number of events as stratigraphic couplets for Zone 1, while a threshold of near 2000 m^3s^{-1} would produce the same number of events as stratigraphic couplets for Zone 4 (Fig. 13).

Comparison of the maximum daily discharge for each water year with Zone 1 unit characteristics revealed patterns related to the highest discharge events and the longest period of low discharge (Fig. 14). The occurrence of the year with the largest daily discharge value (1997) within the time period of deposition is generally consistent with the depth of the thickest medium textured unit. This unit possesses the highest horizon D_{90} and *% coarse* values of Zone 1, although only slightly elevated above several others (Fig. 14). The period of low flows between 1987 and 1992, with maximum annual Q_d values between 2000 and 3000 m^3s^{-1}, was consistent with the lowest Zone 1 units. The Medium units in this position were generally thin (mostly between 1 and 2 cm, with one 5.5 cm unit), while the Fine units were mostly thick

(mostly between 6 and 17.5 cm, with one 3.5 cm unit) (Fig. 14). Fine unit particle size characteristics (D_{90}, *% coarse*) appeared to be insensitive to these discharge patterns.

To examine Zone 4 annual hydrologic and stratigraphic fine/coarser unit couplets, Medium and adjacent Coarse units were combined to form 'Med/Coarse' unit assemblage (Fig. 15). The two years with the highest annual Q_d (1960 and 1963) values may have resulted in the thickest and coarsest unit assemblages, with the lower and thicker of the two corresponding with 1960. Maximum D_{90} and *% coarse* values were almost identical between these two unit assemblages, although 1960 maximum Q_d was 7400 m^3s^{-1} in comparison to 6000 m^3s^{-1} in 1963. In contrast, 1961 and 1962 had maximum Q_d values of 2700 and 2300 m^3s^{-1} respectively and appear to have only resulted in the accretion of a single 5 cm thick Medium unit (Fig. 15).

There were three pieces of evidence for controls of discharge magnitude on stratigraphic characteristics within the second fill sequence (Zone 1, see Figs. 13, 14). (i) There were more years during this deposition period than Medium/Fine unit couplets, while a threshold discharge magnitude of slightly less than 3000 m^3s^{-1} would result in the same number of events and stratigraphic couplets. (ii) The year with the largest discharge event (1997) may have deposited the thickest and coarsest sedimentary unit in Zone 1 (depth 45.5 – 69 cm). (ii) The six year period at the beginning of the record (1987 – 1992) also corresponded with a sequence of relatively thick Fine units at the base of Zone 1.

Abandoned channel fill sequences

The abandoned channel fill sequences of Zones 1 and 4 were typified by (i) sandy, generally unstructured units of lower organic and inorganic carbon content alternating with (ii) finely laminated units of low to no sand with higher OC, $CaCO_3$, ON and OC:ON levels. The frequency of these stratigraphic units closely matched the wet/dry seasonal cycle counts for the time periods of deposition within the error range of chronologic control. The mm-scale laminations found almost universally in the fine horizons was considered diagnostic of tidal deposition rather than fluvial overbank deposits, which would be expected to display a massive fining-up character. Furthermore, the downstream entrance to ropers slough was open throughout the record, contributing to through flow drainage of large hydrologic events. It is with great confidence that these units are identified as recording seasonal scale deposition.

After the 1943 cutoff event, Ropers Slough maintained a higher degree of sediment connectivity with the main channel over a longer period of time, allowing for a more rapid rate of filling and narrowing due a higher degree of bed and coarse suspended sediment entrainment relative to the aftermath of the 1974 cutoff. Although tidal infilling most likely played a role in the first fill sequence, the preponderance of Coarse unit thickness recorded in Zone 4 suggests that fluvial sedimentation was dominant. The later cutoff event was followed by an early transition from main channel, high discharge bed sediments to a sub channel aggrading with sand. After rapid sill/plug bar formation, the EDRS sediment further accreted

through deposition from high water sub-channel flows carrying fluvial suspended sediment, and bidirectional tidal flows redistributing fines during low water conditions.

DISCUSSION

Sediment – discharge relationships

Simple relationships between discharge magnitude and sedimentological characteristics were not found in the reconstruction of the fill progression in Ropers Slough. Although larger floods result in thicker overbank deposits in small systems (Constantine & Pasternack, 2005; Werrity, 2006; Watson *et al.*, 2013) and large systems (Aalto *et al.*, 2008), this would not be generally expected in sediments aggraded under largely through flow conditions. Unlike the basic standing water model for overbank deposits, abandoned channel fills occur under conditions where inundating waters generally remain in motion (Constantine, 2010; Toonen *et al.*, 2012). Also, differences in tidal stage during the incidence of peak sediment discharge may impact the dynamics of water and sediment routing through the abandoned channel, including the induction of backwater effects. Although no consistent event scale hysteresis in suspended sediment concentration has been found for the lower Eel River (Warrick *et al.*, 2013), differences in the timing of peak sediment load relative to peak discharge could also play a role in obscuring a deposition thickness – flood discharge relationship. Intra-unit relationships between discharge and particle size distribution descriptors (e.g., D_{50}, D_{90}, etc.) were also

absent in the latter abandoned channel fill sequence, as little variability in coarse particle sizes was observed. This result is expected for an abandoned channel receiving fluvial inundation from moderate flows ($Q > 2000$ m^3s^{-1}) and above, as Eel River suspended sediment particle size distributions generally did not coarsen with discharge in the moderate to high discharge range.

In contrast, the first abandoned channel fill sequence (Zone 4) displayed potentially more consistent relationships between discharge magnitude and both unit thickness and particle size descriptors. The thickest and coarsest layer may belong to the 1959/60 winter flood season, which had a peak discharge of 9713 m^3s^{-1} and was the largest flood event to deposit sediment in this zone. This coarse unit is more than 7x thicker than any other sandy Zone 4 unit, with a peak D_{90} of 361 µm and 72% sand. A thinner, fining up sequence higher in Zone 4 may have been deposited in 1963, with a peak discharge of 7136 m^3s^{-1}. The peak sand content of this sequence is a coarse unit of only 4 cm thickness, but with a nearly identical sand content and D_{90} values as the 1959/60 unit. Other sandy units in this zone were only 1 to 5 cm thick and much finer with sand contents on the order of 40-55% and D_{90} values from 69 to 190 µm.

Sediment sources

In agreement with the findings of Lario *et al.* (2002) and Watson *et al.* (2013), suspended sediment suite statistical analysis was found to be an informative component of a broader sedimentogical analysis (Fig. 12). The overall pattern of sediment samples in these spaces

further supported the similarity between coarser Zone 3 samples and bed/bedload material, and the finer abandoned channel fills with fluvial materials.

Setting EDRS carbon composition within the context of possible source domains supports the notion that the abandoned channel fill sediments were primarily sourced from Eel River suspended sediment rather than significant littoral/marine contributions. Plotting EDRS the samples with ^{13}C data together with the bounding values reported for Eel River suspended sediment by Goñi et al. (2013) clearly shows that EDRS sediment express almost the same range of $\delta^{13}C$ values as Eel River suspended sediment, with no consistent variation between Zones (Fig. 16a). When plotted in $\delta^{13}C$ vs. ON:OC space, it becomes clear that EDRS sediment primarily deviate from Eel River suspended sediment values due to the addition of C_3 vascular plant material, most likely from the C_3 sedges and rushes common to this part of the estuary (Fig. 16b). The deposited sediments that deviate most from Eel River suspended sediment are those from Zone 1 – which is consistent with plant detritus from emergent vegetation. Closer examination also shows some separation of between stratigraphic zones, with Zone 1 horizons generally lower in $\delta^{13}C$ and ON:OC values – again consistent with vascular plant detritus, while Zone 4 values were generally higher. The highest of these Zone 4 values, in addition to the few high values from Zones 2 and 3, were also among the coarsest samples. Conversely, Goñi et al. (2013) found that the Eel River suspended sediment pool deviated toward decreased $\delta^{13}C$ and ON:OC values with increased discharge, although little change occurred with increased

discharge above ~ 800 m^3s^{-1}. Most of the sediment moved by the Eel River occurs during higher discharges (Brown and Ritter, 1971; Warrick *et al.*, 2013, Warrick, 2014).

Although not definitive proof, these comparisons do corroborate the notion that some of the coarser sediment deposited earlier in the record were transported by smaller flows under more open, hydrologically connected conditions. In contrast, tidally reworked sediment may in part bear the signature of the larger body of sediment transported into the Eel River Estuary by higher discharge events. In both cases, the channel fill sequences appear to be dominated by Eel River suspended and bedload sediments.

Mechanisms

What caused the differences in narrowing rates and stratigraphic characteristics between the first and second abandoned channel sequences? Both sequences began as main channels that experienced abandonment through chute cut-offs of identical diversion angles (~ 67°) and cutoff ratios. In both cases the EDRS site was positioned about the same distance from the RSC/Ropers Slough bifurcation (Node 2). However, the first abandonment resulted in a much more rapid narrowing of Ropers Slough, and after 15 to 20 years of narrowing and shoaling the first abandoned channel fill produced wet season fluvial deposits that were generally sandier, coarser, and thicker than those found in the second fill sequence. In fact, the fluvial deposits of

the first fill sequence more closely resemble the earliest units deposited just after the second abandonment.

Differences in stratigraphy between the first and second abandoned channel fill sequences were due to differences in some combination of (i) external forcing factors such as flood and tidal magnitudes, and sediment load and (ii) internal factors such as local bed/channel geometry, and their effects on local hydraulics and sediment transport (Toonen *et al.*, 2012). Large flooding events during the winters of 1955/56 and 1964/65 with return intervals of 100 and 200 years, respectively, are known to have augmented suspended sediment loads, an effect that has decreased over the subsequent decades (Warrick *et al.*, 2013). Higher sediment loads during the 1950s and 1960s may be responsible in part for the rapid filling of the first sequence, however, much of the observed narrowing occurred by 1948, well before the 1956 event. Sediment loads in the 1940s may have also been very high, but there are no suspended sediment data from this time period (Warrick *et al.*, 2013). Furthermore, the largest discharge event at Scotia between the first abandonment and 1948 was only 6768 m^3s^{-1} (about 7500 m_3s_{-1} to the estuary), or about a 5 year return interval flow.

Alternatively, the first and second abandonment sequences were influenced by the position of the entrance to Ropers Slough relative to RSC complex meander bend morphology. While the factors of accommodation space and higher sediment load may have some bearing on the rapidity of first sequence fill, local channel curvature is perhaps the most compelling

contributing factor. The massive floods of 1955 and 1964 could not have influenced the early narrowing of the first abandonment between 1943 and 1948. Furthermore, accommodation space must have been substantially reduced by the time that the lowest EDRS strata were deposited in the late 1950s. Channel curvature controls on water and sediment apportioning, however, would have been operational over the entirety of each fill period.

The meander bends associated with the bifurcation at the entrance Ropers Slough were accreting point bars. Bed sediment can be expected to behave differently in the entrance region of each bifurcate depending on its location relative to the upstream meander bend, particularly if there is an inner bend that is accreting a point bar (Kleinhans, 2008; Seminara, 2001). When this is the case, others have found that the bifurcate extending from the inner bank would be expected to have more bed accreted in the mouth region than the bifurcate extending from the outer bank (Hooke, 1995; Constantine *et al.*, 2010; Toonen *et al.*, 2012). Indeed, the entrances of bifurcates located on inner bends, namely the RSC complex from 1940 to ~1965, and Ropers Slough from 1974 to the present appeared to rapidly accrete point bars (see Fig. 3). Conversely, the Ropers Slough entrance from 1940 to ~1965 was located on the outer bend, and did not appear to seal off due to plug bar formation over time (see Fig. 3).

New conceptual model evaluation

Modification of the generic fluvial model for abandoned channel stratigraphic architecture to include seasonal scale tidal deposits appeared to be well supported by the case of Ropers Slough (Figure 17). Both of the abandoned channel fill sequences examined in this study recorded periods of fluvial and tidal deposition with almost seasonal resolution. This contrasts sharply with discreet flood based laminations found in scenarios of overbank deposition, such as oxbow lakes, which record the frequency of floods above overbank thresholds that can range from event to decadal frequencies. Also, overbank settling deposits tend to display massive fining up sequences rather than the seasonal couplets of coarser fluvial, and fine laminated tidal deposits found in the Ropers Slough fill.

Previous generic mechanisms for abandoned channel fill evolution were supported by the differences in both geomorphic and stratigraphic evolution between the first and second fill sequences. Differences in the topographic steering of bedload and water, and plug bar formation rates related to the position of the abandoned channel mouth relative to meander morphology led to the expected directions of difference in channel narrowing and sediment texture. Slower plug bar formation during the first fill sequence may have led to generally lower threshold discharge values required for inundation of Ropers Slough than those required after the rapid plug bar formation experienced over the second fill sequence.

Additional large scale planform investigations of numerous abandoned channels experiencing wet/dry seasonality along a continuum of tidal influence is required to address the role of tidal

pumping on channel reoccupation behavior. In depth reductive studies on the hydraulics, sediment transport and erosional dynamics of tidal rivers are also critical to understanding the relative roles of the forcing factors speculated upon here. Tidal channel fills are widespread and important geomorphic phenomena, and it is critical that their functionality and depositional characteristics are more fully understood (van den Berg *et al*., 2007). Most of these environments in developed nations such as the U.S. are severely impacted by human activity, and will increasingly be the target of restoration activities, which will require generic and reductionist understanding in order to be successful. Furthermore, the deposits within the abandoned channels have much to offer communities interested in historical characterization of coastal, estuarine and integrated watershed environmental signals, as they can potentially capture high resolution records of fluvial and tidal activity. There is currently great interest in mapping tsunami and rapid subsidence deposits related to large ground shaking events along active margins (Atwater, 1992; Shennan, *et al.*, 1996; Dawson and Shi, 2000; Vott *et al.*, 2014). Accurate identification of such deposits in fluvial estuaries can be complicated by their similarity to abandoned channel fills, particularly when an intensive characterization of the estuary fill architecture at large is not available. Thus, developing a clear stratigraphic framework that unites abandoned channel fills with the tidal environment would be an important step toward increasing the understanding and utility of these widespread features of coastal sedimentary deposits.

CONCLUSIONS

Abandoned channel fill sequences in tidally influenced river reaches subjected to pronounced wet/dry seasons seem to follow most of the same generic pathways of non-tidal abandoned channel fills, with the addition of tidal effects on deposition and scour. Fluvial units from Ropers Slough abandoned channel fill sequences appear to have been derived primarily from suspended sediment. However, higher connectivity with the main northern channel (RSC complex) during the first abandonment sequence appears to have allowed for coarser material, perhaps bed or highly stratified coarse suspended sediment, to enter the slough during larger discharge events. Further evidence was found for the control of channel meander bend morphology relative to abandoned channel entrance position on plug bar formation. Inner bend position of the channel entrance seems to have resulted in rapid plug bar formation during the latest abandonment sequence of Ropers Slough. This resulted in a slower progression of channel narrowing, and thinner fluvial strata that did not respond to discharge magnitude in terms of deposition thickness or coarseness. Decreasing sediment load and tidal prism in the Eel River over the time period of accretion may also have influenced this difference, but this issue remains unclear.

Tidally influenced abandoned channel fills in dry summer climates diverge from the generic model developed for rivers experiencing only unidirectional flow by generating the following structures:

1. Fine/coarse textured unit couplets that correspond to dry season tidal deposition and wet season fluvial deposition, respectively.

2. Fine horizons displayed mm-scale, sub-seasonal laminations indicative of tidal deposition found in through flow channels, in contrast to the the seasonal scale laminations found in fully disconnected oxbow lakes receiving only large overbank events.

3. Tidal deposits contained increased carbonate levels during both fill sequences and may have transitioned to more depressed $\delta^{13}C$ and ON:OC values during the second fill sequence due to higher discharge event signatures.

ACKNOWLEDGEMENTS

This research was primarily funded by the National Science Foundation under award No. 0628385. Support was also received from the Hydrologic Sciences Graduate Group at the University of California at Davis, a Jastro Shields graduate research award, and the USDA National Institute of Food and Agriculture, Hatch project number #CA-D-LAW-7034-H. The radiocarbon work at NOSAMS was supported in part by the NSF Cooperative Agreement number, OCE-0753487. We thank Dr. Erik Wisner and the University of California at Davis Veterinary Medical Center Small Animal Clinic staff for assistance and support with x-radiography of the sediment core. Any opinions, findings, and conclusions or recommendations expressed in this material are those of the authors and do not necessarily reflect the views of

the funding institutions. We thank Peter Barnes, Sarah Greve, Duyen Ho, Olivia Oseguera, Drisanna Watson and Sonja Gray for field and laboratory assistance, as well as Dawn Sumner and Rocko Brown for suggestions that significantly improved this manuscript.

REFERENCES

Aalto, R., Lauer, J.W. and **Dietrich, W.E.** (2008) Spatial and temporal dynamics of sediment accumulation and exchange along Strickland River floodplains (Papua New Guinea) over decadal-to-centennial timescales. *J. Geophys. Res*., **113**, F01S04. doi:10.1029/2006JF000627.

Allen, J.R.L. (1965) A review of the origin and characteristics of recent alluvial sediments. *Sedimentology*, **5**, 89-191.

Andrews, E.D., Antweiler, R.C., Neiman, P.J. and **Ralph, F.M.** (2004) Influence of ENSO on flood frequency along the California coast. *Journal of Climate*, **17**, 337-348.

Aslan, A., Autin, W.J. and Blum, M.D. (2005) Causes of river avulsion: Insights from the late Holocene avulsion history of the Mississippi River, USA. *Journal of Sedimentary Research*, **75,** 650-664.

Atwater, B.F. (1992) Geologic evidence for earthquakes during the past 2000 years along the Copalis River, southern coastal Washington. *J. Geophys. Res.-Solid Earth*, **97**, 1901-1919.

Blair, N.E., Leithold, E.L. and **Aller, R.C.** (2004) From bedrock to burial: the evolution of particulate organic carbon across coupled watershed-continental margin systems. *Mar. Chem.*, **92**, 141-156.

Boles, G.L., Clawson, R.F. and **Lallatin, R.D.** (1977) Some physical, chemical, and biological characteristics of the Eel River Estuary. California Department of Water Resources. Memorandum. pp. 100.

Blott, S.J. and **Pye, K.** (2001) GRADISTAT: A grain size distribution and statistics package for the analysis of unconsolidated sediments. *Earth Surf. Process. Landf*., **26**, 1237-1248.

Brown, W.M. and **Ritter, J.R.** (1971) Sediment transport and turbidity in the Eel River basin, California. U.S. Geological Survey Water Supply Paper 1986. pp.70.

Buchholz, B.A. (2009) Bomb-Pulse Dating, in *Wiley Encyclopedia of Forensic Science*. John Wiley & Sons, Ltd., DOI: 10.1002/9780470061589.fsa606.

California Department of Fish and Game (CDFW) (2010) DRAFT Lower Eel River watershed assessment. CDFG Coastal Watershed Planning and Assessment Program, Fortuna, CA.

Cannata, S. and **Hassler T.** (1995) Spatial and temporal distribution and utilization patterns of juvenile anadromous salmonids of the Eel River estuary, June 1994–September 1995. IN: J. Duncan-Vaughn, ed., Proceedings of the Thirteenth Annual Salmonid Restoration Federation Conference, February 23–26, 1995, Santa Rosa, CA.

Citterio, A. and **Piégay H.** (2009) Overbank sedimentation rates in former channel lakes: characterization and control factors. *Sedimentology*, **56**, 461–482.

Constantine, J.A., Dunne, T., Piégay, H. and **Kondolf, G.M.** (2010) Controls on the alluviation of oxbow lakes by bed-material load along the Sacramento River, California. *Sedimentology*, **57**, 389-407.

Constantine, J.A., Pasternack, G.B. and **Johnson, M.L.** (2005) Logging effects on sediment flux observed in a pollen-based record of overbank deposition in a northern California catchment. *Earth Surf. Process. Landf.*, **30**, 813-821.

Dawson, A.G. and **Shi, S.Z.** (2000) Tsunami deposits. *Pure Appl. Geophys.*, **157**, 875-897.

Downie, S.T. and **Lucey K.P.** (2005) Salt River watershed assessment. California Department of Fish and Game, Coastal Watershed Planning and Assessment Program, Fortuna, CA.

Fisk, H.N. (1947) Fine grained alluvial deposits and their effects on Mississippi River activity, Vols 1 & 2. Mississippi River Commission, Vicksburg, MS.

Folk, R.L. (1974) *Petrology of Sedimentary Rocks.* Hemphill, Austin, TX, pp. 184.

Fry, B., Brand, W., Mersch, F., Tholke, K. and **Garritt, R.** (1992) Automated analysis system for coupled delta-C-13 and delta N-15 measurements. *Analytical* Chemistry, **64**, 288–291.

Ghinassi, M. (2011) Chute channels in the Holocene high-sinuosity river deposits of the Firenze plain, Tuscany, Italy. *Sedimentology*, **58**, 618–642. http://dx.doi.org/10.1111/ j.1365-3091.2010.01176.x.

Goñi, M.A., Hatten, J.A., Wheatcroft, R.A. and Borgeld, J.C. (2013) Particulate organic matter export by two contrasting small mountainous rivers from the Pacific Northwest, USA. *Journal of Geophysical Research-Biogeosciences*, **118,** 112-134.

Goñi, M., Yunker, M., Macdonald, R. and **Eglinton, T.** 2000. Distribution and sources of organic biomarkers in arctic sediments from the Mackenzie River and Beaufort Shelf. *Marine Chemistry*, **71**, 23–51.

Goñi, M., Yunker, M., Macdonald, R. and **Eglinton, T.** (2005) The supply and preservation of ancient and modern components of organic carbon in the Canadian Beaufort Shelf of the Arctic Ocean. *Marine Chemistry*, **93**, 53– 73.

Gray, A.B., Pasternack, G.B. and **Watson, E.B.** (2010) Hydrogen peroxide treatment effects on the particle size distribution of alluvial and marsh sediments. *Holocene*, **20**, 293-301.

Haley, R. (1970) Changes in the Eel River Estuary and its Fisheries. California Department of Fish and Game, Memorandum. pp. 7.

Haltiner, J. and Williams, P.B. (1987) Slough channel design in salt marsh restoration. In: *Eighth Annual Meeting of Wetland Scientists*, pp. 125-130, Seattle.

Helsel, D.R. and **Hirsch, R.M.** (2002) Statistical Methods in Water Resources—Hydrologic Analysis and Interpretation. *U.S. Geological Survey Techniques of Water-Resources Investigations*, book 4, chap. A3, Washington, DC, pp. 510.

Hoek, W.Z., Minderhoud, P.S.J., Cohen, K.M., Erkens, G. and **Toonen, W.H.J.** (2011) Towards a Decadal Flood Record of the River Rhine Over the Last 7000 Years, Abstract volume: Quaternary Research Association, Annual Discussion Meeting.

Hooke, J.M. (1995) River channel adjustment to meander cutoffs on the River Bollin and River Dane, northwest England. *Geomorphology*, **14**, 235-253.

Howard, A.D. (1996) Modeling channel evolution and floodplain morphology, in: Anderson, M.G., Walling, D.E., Bates, P.D. (Eds.), *Floodplain Processes*. John Wiley and Sons Ltd., Chichester, UK, pp. 15–65.

Hughes, M.L., McDowell, P.F. and **Marcus, W.A.** (2006) Accuracy assessment of georectified aerial photographs: Implications for measuring lateral channel movement in a GIS. *Geomorphology*, **74**, 1-16.

Kelsey, H.M., (1980) A sediment budget and an analysis of geomorphic process in the Van-Duzen river basin, north coastal California, 1941-1975 - SUMMARY. *Geol. Soc. Am. Bull,.* **91**, 190-195.

Kleinhans, M.G., Cohen, K.M., Hoekstra, J. and **IJmker, J.M.** (2011) Evolution of a bifurcation in a meandering river with adjustable channel widths, Rhine delta apex, The Netherlands. *Earth Surface Processes and Landforms*, **36** (15), 2011-2027.

Kleinhans, M.G., Ferguson, R.I., Lane, S.N. and Hardy, R.J. (2013) Splitting rivers at their seams: bifurcations and avulsion. *Earth Surface Processes and Landforms*, **38,** 47-61.

Kleinhans, M.G., Jagers, H.R.A., Mosselman E. and **Sloff, C.J.** (2008) Bifurcation dynamics and avulsion duration in meandering rivers by one-dimensional and three-dimensional models. *Water Resources Research*, **44**, W08454.

Kleinhans, M.G., Schuurman, F., Bakx, W., and **Markies, H.** (2009) Meandering channel dynamics in highly cohesive sediment on an intertidal mud flat in the Westerschelde estuary, the Netherlands. *Geomorphology*, **105**, 261-276.

Kleinhans, M.G., Weerts, H.J.T. and **Cohen, K.M.** (2010) Avulsion in action: Reconstruction and modelling sedimentation pace and upstream flood water levels following a Medieval tidal-river diversion catastrophe (Biesbosch, The Netherlands, 1421-1750 AD). Geomorphology, **118**, 65-79.

Lario, J., Spencer, C., Plater, A.J., Zazo, C., Goy, J.L., and **Dabrio, C.J.** (2002) Particle size characterization of Holocene back-barrier sequences from North Atlantic coasts (SW Spain and SE England). *Geomorphology*, **42**, 25-42.

Lewis, G.W. and **Lewin, J.** (1983) Alluvial cutoffs in Wales and the Borderlands. In: Collinson, J.D., Lewin, J. (Eds.), *Modern and Ancient Fluvial Systems*. Blackwell Publishing Ltd., Oxford, UK, pp. 145–154. http://dx.doi.org/10.1002/9781444303773.ch11.

Li, W.H. (1992) The late Holocene stratigraphy of the Eel River delta. In: *Field guide to the late Cenozoic subduction tectonics and sedimentation of northern coastal California* (Eds G.A. Carver and K.R. Aalto). pp. 55-57 GB-71. Pacific section. American Association of Petroleum Geologists.

Mackey, B.H. and **Roering, J.J.** (2011) Sediment yield, spatial characteristics, and the long-term evolution of active earthflows determined from airborne LiDAR and historical aerial photographs, Eel River, California. *Geol. Soc. Am. Bull.*, **123**, 1560-1576.

Madej, M.A., Bundros, G. and **Klein, R.** (2012) Assessing effects of changing land use practices on sediment loads in Panther Creek, North Coastal California. In: *Proceedings of Coast Redwood Forests in a Changing California: A Symposium for Scientists and Managers* (Eds R.B. Standiford, T.J. Weller, D.D. Piirto, J.D. Stuart). Gen. Tech. Rep. PSW-GTR-238. Pacific Southwest Research Station, Forest Service, U.S. Department of Agriculture, Albany, CA.

McLaughlin, R. J., Blake, M. C. J., Griscom., A., Blome, C.D. and **Murchey, B.** (1988) Tectonics of Formation, Translation, and Dispersal of the Coast Range Ophiolite of California. *Tectonics*, **7**(5), 24.

Mount, N.J., Louis, J., Teeuw, R.M., Zukowskyj, P.M. and **Stott, T.** (2003) Estimation of error in bankfull width comparisons from temporally sequenced raw and corrected aerial photographs. *Geomorphology*, **56**, 65-77.

Nittrouer, C.A. (1999) STRATAFORM: overview of its design and synthesis of its results. *Mar. Geol.*, **154**, 3-12.

Ostermann, D.R., Karbott, D. and **Curry, W.B.** (1990) Automated system to measure the carbonate concentration of sediments. WHOI Tech. Rept., 90-03, 1–17.

Puckett, L.K. (1977) The Eel River Estuary – Observations on Morphometry, Fishes, Water Quality, and Invertebrates. California Department of Fish and Game. Memorandum Report. pp. 27.

Puckridge, J.T., Walker, K.F. and **Costelloe, JF.** (2000) Hydrological persistence and the ecology of dryland rivers. *Regulated Rivers-Research & Management*, **16**, 385-402. DOI: 10.1002/1099-1646(200009/10)16:5<385::aid-rrr592>3.3.co;2-n

Rafter, T.A. and **Fergusson, G.J.** (1957) The atom bomb effect – recent increase of carbon-14 content of the atmosphere and biosphere, *Science*, **126**, 557–558.

Reimer, P.J., Bard, E., Bayliss, A., Beck, J.W., Blackwell, P.G., Ramsey, C.B., Buck, C.E., Cheng, H., Edwards, R.L., Friedrich, M., Grootes, P.M., Guilderson, T.P., Haflidason, H., Hajdas, I., Hatte, C., Heaton, T.J., Hoffmann, D.L., Hogg, A.G., Hughen, K.A., Kaiser, K.F., Kromer, B., Manning, S.W., Niu, M., Reimer, R.W., Richards, D.A., Scott, E.M., Southon, J.R., Staff, R.A., Turney, C.S.M. and **van der Plicht, J.** (2013) INTCAL13 and MARINE13 Radiocarbon age calibration curves 0-50,000 years cal BP. *Radiocarbon*, **55**, 1869-1887.

Robinson, A.H.W. (1960) Ebb-flood Channel Systems in Sandy Bays and Estuaries. *Geography*, **45**, 183-199.

Schlosser, S. and **Eicher, A.** (2012) The Humboldt Bay and Eel RiverEstuary Benthic Habitat Project. California Sea Grant Publication T-075. pp. 246.

SCS (1989) Salt River Watershed Workplan, including the Lower Eel River, Delta, and Estuary Workplan. US Department of Agriculture, Soil Conservation Service, Eureka, CA.

Seminara, G., Zolezzi, G., Tubino, M. and **Zardi, D.** (2001) Downstream and upstream influence in river meandering. Part 2. Planimetric development. *J. Fluid Mech.*, **438**, 213-230.

Shennan, I., Long, A.J., Rutherford, M.M., Green, F.M., Innes, J.B., Lloyd, J.M., Zong, Y. and **Walker, K.J.** (1996) Tidal marsh stratigraphy, sea-level change and large earthquakes .1. A 5000 year record in Washington, USA. Quat. Sci. Rev., **15**, 1023-1059.

Shields, F.D. Jr and **Abt, S.R.** (1989) Sediment deposition in cutoff meander bends and implications for effective management. *Regulated Rivers Res. Manage.*, **4**, 381–396.

Sloan, J., Miller, J.R. and **Lancaster, N.** (2001) Response and recovery of the Eel River, California, and its tributaries to floods in 1955, 1964, and 1997. *Geomorphology*, **36**, 129-154.

Smith N.D., Slingerland R.L., Perez-Arlucea M. and **Morozova G.S.** (1998) The 1870s avulsion of the Saskatchewan River. Canadian Journal of Earth Sciences, **35**, 453–466.

Sommerfield, C.K., Drake, D.E. and **Wheatcroft, R.A.** (2002) Shelf record of climatic changes in flood magnitude and frequency, north-coastal California. *Geology*, **30**, 395-398.

Sommerfield, C.K. and **Wheatcroft, R.A.** (2007) Late Holocene sediment accumulation on the northern California shelf: Oceanic, fluvial, and anthropogenic influences. *Geol. Soc. Am. Bull.*, **119**, 1120-1134.

Sommerfield, C.K., Ogston, A.S., Mullenbach, B.L., Drake, D.E., Alexander, C.R., Nittrouer, C.A., Borgeld, J.C., Wheatcroft, R.A. and Leithold, E.L. (2007) Oceanic dispersal and accumulation of river sediment. In: *Continental Margin Sedimentation: From Sediment*

Transport to Sequence Stratigraphy (Eds C.A. Nittrouer, J.A. Austin, M.E. Field, J.H. Kravitz, J.P.M. Syvitski and P.L. Wiberg), *Special Publications of the International Association of Sedimentologists*, **37**, pp. 157-212.

Sun, T., Meakin, P., Jossang, T. and **Schwarz, K.** 1996. A simulation model for meandering rivers. *Water Resour. Res.*, **32**, 2937-2954.

Stouthamer E. (2005) Reoccupation of channel belts and its influence on alluvial architecture in the Holocene Rhine-Meuse delta, the Netherlands. In River Deltas: Concepts, Models, and Examples (Eds L. Giosan, J.P. Bhattacharya), SEPM, Special Publication 83. SEPM (*Society for Sedimentary Geology*): Tulsa, OK; 319–339.

Stuiver, M. and **Polach, H.A.** (1977) Reporting of C-14 data - discussion. *Radiocarbon*, **19**, 355-363.

Tanner, W.F. (1991) Suite statistics: the hydrodynamic evolution of the sediment pool. In: *Principles, Methods and Applications of Particle Size Analysis* (Ed J.P.M. Syvitski), pp. 225-236. Cambridge University Press, Cambridge, UK.

Tanner, W.F. (1995) William F. Tanner on environmental clastic granulometry. Florida Geological Survey Special Publication No. 40, 163 pp. ISSN 0085-0640.

Toonen, W.H.J., Kleinhans, M.G. and **Cohen, K.M.** (2012) Sedimentary architecture of abandoned channel fills. *Earth Surf. Process. Landf.,* **37**, 459-472.

U.S. Geological Survey Earth Explorer (USGS EarthExplorer) (2014) http://earthexplorer.usgs.gov/ (last accessed: 3/2014)

U.S. Geological Survey National Water Information System (USGS NWIS) (2014) http://waterdata.usgs.gov/nwis/sw (last accessed: 03/2014).

van den Berg, J.H., Boersma, J.R. and van Gelder, A. (2007) Diagnostic sedimentary structures of the fluvial-tidal transition zone - Evidence from deposits of the Rhine and Meuse. *Netherlands Journal of Geosciences-Geologie En Mijnbouw*, **86,** 287-306.

Van Kirk, S. (1996) Historical accounts of the Lower Eel (Wiyot) River navigation, fisheries, "angry waters", land use, and the river environment 1850–1995. Prepared by Trinity Associates, Arcata, CA.

van Veen, J., van der Spek, A.J.F., Stive, M.J.F. and **Zitman, T.** (2005) Ebb and flood channel systems in the Netherlands tidal waters. Journal of Coastal Research, **21**, 1107-1120.

Vott, A., Reicherter, K. and **Papanikolaou, I.** (2013) Reconstructing and modeling palaeotsunami events by multi-proxy geoscientific analyses. *Z. Geomorphol.*, **57**, 1-4.

Warrick, J.A., Madej, M.A., Goñi, M.A. and **Wheatcroft, R.A.** (2013) Trends in the suspended-sediment yields of coastal rivers of northern California, 1955-2010. *J. Hydrol.*, **489**, 108-123.

Warrick, J.A. (2014) Eel River margin source-to-sink sediment budgets: Revisited. *Marine Geology*, **351**, 25-37.

Wentworth CK. (1922) A scale of grade and class terms for clastic sediments. *Journal of Geology*, **30**, 377–392.

Werritty, A., Paine, J.L., Macdonald, N., Rowan, J.S. and **McEwen, L.J.** (2006) Use of multi-proxy flood records to improve estimates of flood risk: Lower River Tay, Scotland. *Catena*, **66**, 107-119.

Watson, E.B., Pasternack, G.B., Gray, A.B., Goni, M. and **Woolfolk, A.M.** (2013) Particle size characterization of historic sediment deposition from a closed estuarine lagoon, Central California. *Estuar. Coast. Shelf Sci.*, **126**, 23-33.

Wheatcroft, R.A., Sommerfield, C.K., Drake, D.E., Borgeld, J.C. and **Nittrouer, C.A.** (1997) Rapid and widespread dispersal of flood sediment on the northern California margin. *Geology*, **25**, 163-166.

Zinger, J.A., Rhoads, B.L. and Best, J.L. (2011) Extreme sediment pulses generated by bend cutoffs along a large meandering river. *Nature Geosci*, **4,** 675-678.

Table 1. Aerial photograph source data

Date	Agency[b]	Resolution (m)	Spatial distortion (m)[c]	GCP[d]
7/27/2009	NOAA	0.50	-	-
6/29/2005	USDA, NAIP	1.00	-	-
9/3/1998	USGS	3.49	0.47	14
6/15/1993	USGS	3.23	0.49	>10
4/28/1989	USGS	4.06	0.08	>10
8/28/1985	USGS	2.24	0.10	11
7/8/1982	USGS	6.90	0.67	>10
6/27/1980	USGS	7.11	4.33	14
5/29/1979	USGS	8.16	1.73	13
5/8/1978	USGS	5.69	0.91	13
1/4/1977	USGS	6.51	0.71	11
4/29/1974	USGS	6.64	0.89	14
4/3/1974	USGS	7.47	1.39	12
1/21/1974	USGS	6.19	0.88	12
4/4/1973	USGS	5.31	0.83	13
7/15/1972	USGS	1.00	0.55	13
summer, 1965[a]	HBHRCD	0.70	4.70	30
9/13/1956	USGS	1.10	1.46	16
summer, 1948[a]	HBHRCD	0.70	2.58	26
12/13/1940	USGS	1.09	0.82	14

[a]The 1965 and 1948 high resolution mosaics were collected over an undetermined time period durring the respective summer seasons.

[b]The Agencies are: NOAA= National Oceanographic and Atmospheric Administration, USDA; NAIP = U.S. Department of Agriculture, National Agriculture Imagery Program; USGS = U.S. Geological Survey.

[c]Spatial distortion reported as the maximum if multiple digital photographs used for a given date

[d]GCP = Georeferenced control points. The values listed indicate the minimum number of control points if multiple digital photographs were used for a given date.

Table 2. EDRS depositional environments

Date	Depositional Environment	Ropers[a] Entrance
12/13/1940	Main channel	-
summer, 1948	Abandoned	Outer bank
9/13/1956	Abandoned	Outer bank
summer, 1965	Main channel	Outer bank
7/15/1972	Main channel	-
4/4/1973	Main channel	-
1/21/1974	Main channel	-
4/29/1974	Main channel	Inner Bank
1/4/1977	Abandoned	Inner Bank
5/8/1978	Abandoned	Inner Bank
5/29/1979	Abandoned	Inner Bank
6/27/1980	Abandoned	Inner Bank
7/8/1982	Abandoned	Inner Bank
8/28/1985	Abandoned	Inner Bank
4/28/1989	Abandoned	Inner Bank
6/15/1993	Abandoned	Inner Bank
9/3/1998	Abandoned	Inner Bank
6/29/2005	Emergent marsh	Inner Bank
6/27/2009	Emergent marsh	Inner Bank

[a]The position of the upstream entrance to Ropers Slough (E. Ropers Mouth) relative to the meander morphology of the RSC complex.

Table 3. Radiocarbon measurements

					2σ year ranges[b]			
Mean Depth (cm)	Sample ID[a]	$F^{14}C$	$F^{14}C$ Error	$\delta^{13}C$	Cal Year AD	Probability	Cal Year AD	Probability
62.5	CAMS-163329	1.118801	0.0054	-25.93	1957.8 : 1958.6	0.067	**1993.1 : 1998.7**	0.933
166.5	CAMS-163330	1.214663	0.0035	-27.79	1959.0 : 1961.5	0.341	**1983.0 : 1986.2**	0.659
252.5	CAMS-163331	1.387876	0.0078	-25.93	**1962.5 : 1962.8**	0.143	1973.3 : 1976.5	0.857
302	CAMS-163332	1.072338	0.0041	-25.93	**1957.1 : 1957.8**	0.086	2002.1 : 2007.2	0.914
302	OS-71195	1.064300	0.0021	-27.24	**1956.9 : 1957.6**	0.104	2004.0 : 2009.5	0.896

[a]Identification code prefixes as follows: CAMS = Lawerence Livermore National Laboratory Center for Accelerator Mass Spectrometry, OS = National Ocean Sciences Accelerator Mass Spectrometry Facility.

[b]Year ranges and associated probabilities are the product of calibrating $F^{14}C$ with $F^{14}C$ error using the CaliBomb model of post bomb pulse ^{14}C levels in zone NH2. This produces a low probability, 'old' distribution of dates, and a high probability 'young' distribution, due to the rapid rate of ^{14}C increase in the atmosphere at the beginning of the bomb pulse, and the relatively slower decline in ^{14}C levels after the mid 1960s. Most likely year ranges indicated in bold were chosen with consideration for stratigraphic sequence and the time series of planform geomorphology.

Table 4. Comparisons of EDRS mean particle size distribution characteristics[a].

Particle size distribution characteristics by horizon type an zone.											
Horizon type	Zones	1° Mode	Sorting	Skewness	Kurtosis	D_{10}	D_{50}	D_{90}	% Clay	% Silt	% Coarse[b]
Fine	Z1 vs. Z4	Eq.	Eq.	*	*	Eq.	Eq.	Eq.	Eq.	Eq.	-
Sandy	Z1 vs. Z2	**	***	**	**	***	***	***	***	***	***
Sandy	Z1 vs. Z3	***	***	Eq.	*	**	**	*	***	***	***
Sandy	Z1 vs. Z4	***	Eq.	Eq.	*	***	***	***	Eq.	***	***
Sandy	Z2 vs. Z3	***	**	Eq.	Eq.	**	**	*	Eq.	**	*
Sandy	Z2 vs. Z4	Eq.	Eq.	Eq.	Eq.	Eq.	Eq.	Eq.	*	Eq.	Eq.
Sandy	Z3 vs. Z4	**	**	Eq.	*	**	**	*	*	**	**

[a]Results for one sided T-tests listed as follows: (Eq.) indicates the H_0 of equivalent means was not rejected (P-value > 0.05), (*) for P-values < 0.05, (**) for P-values < 0.01, (***) for P-values < 0.001.

[b]The descriptor % coarse is the sum of % sand and % gravel.

Table 5. EDRS mean carbon content characteristics[a].

Carbon characteristics by horizon type an zone.						
Horizon type	Zone	% OC	% $CaCO_3$	% ON	OC:ON	$\delta^{13}C$ (per mil)
Fine	Z1	1.22 ± 0.84	0.84 ± 0.70	0.09 ± 0.06	15.7 ± 1.8	-26.0 ± 0.4
Fine	Z4	0.76 ± 0.08	1.02 ± 0.44	0.07 ± 0.01	13.5 ± 1.7	-25.6 ± 0.1
Sandy	Z1	0.84 ± 0.26	0.60 ± 0.61	0.06 ± 0.01	16.7 ± 2.5	-26.2 ± 0.3
Sandy	Z2	0.50 ± 0.23	0.16 ± 0.25	0.04 ± 0.01	13.2 ± 2.4	-25.7 ± 0.3
Sandy	Z3	0.34 ± 0.19	0.13 ± 0.20	0.03 ± 0.01	13.5 ± 3.6	-25.6 ± 0.4
Sandy	Z4	0.63 ± 0.40	0.51 ± 0.60	0.05 ± 0.02	15.0 ± 4.6	-25.5 ± 0.8
Carbon characteristics by facies unit.						
Facies Unit[b]		% OC	% $CaCO_3$	% ON	OC:ON	$\delta^{13}C$(per mil)
Fine		1.13 ± 0.77	0.88 ± 0.66	0.09 ± 0.06	15.3 ± 1.9	-25.9 ± 0.4
Medium		0.79 ± 0.28	0.55 ± 0.57	0.06 ± 0.01	16.2 ± 2.7	-26.0 ± 0.5
Coarse		0.41 ± 0.35	0.21 ± 0.51	0.03 ± 0.01	13.4 ± 4.8	-25.8 ± 0.7
Very Coarse		0.20 ± 0.06	0.06 ± 0.11	0.02 ± 0.003	12.1 ± 3.7	-25.4 ± 0.05

[a]Results reported as mean +/- 1 standard deviation.

[b]Facies units refer to all horizons with the indicated ranges of % coarse: Fine = (0-7%); Medium = (7-50%); Coarse = (>50% no gravel); Very Coarse = (>50% w/gravel).

Table 6. Comparisons of EDRS carbon content characteristics[a].

Carbon characteristics by horizon type an zone.						
Horizon type	Zones	% OC	% $CaCO_3$	% ON	OC:ON	$\delta^{13}C$
Fine	Z1 vs. Z4	***	Eq.	**	***	**
Sandy	Z1 vs. Z2	***	***	***	***	**
Sandy	Z1 vs. Z3	***	***	***	***	Eq.
Sandy	Z1 vs. Z4	**	Eq.	**	*	Eq.
Sandy	Z2 vs. Z3	*	Eq.	**	Eq.	Eq.
Sandy	Z2 vs. Z4	Eq.	**	Eq.	Eq.	Eq.
Sandy	Z3 vs. Z4	**	**	**	Eq.	Eq.
Carbon characteristics by facies unit.						
Facies Unit[b]		% OC	% $CaCO_3$	% ON	OC:ON	$\delta^{13}C$
Fine	vs. Medium	***	***	***	**	Eq.
Fine	vs. Coarse	***	***	***	*	Eq.
Fine	vs. Very Coarse	***	***	***	*	***
Medium	vs. Coarse	***	**	***	**	Eq.
Medium	vs. Very Coarse	***	***	***	**	***
Coarse	vs. Very Coarse	**	Eq.	***	Eq.	Eq.

[a]Results for one sided T-tests listed as follows: (Eq.) indicates the H_0 of equivalent means was not rejected (P-value > 0.05), (*) for P-values < 0.05, (**) for P-values < 0.01, (***) for P-values < 0.001.

[b]Facies units refer to all horizons with the indicated ranges of % coarse: Fine = (0-7%); Medium = (7-50%); Coarse = (>50% no gravel); Very Coarse = (>50% w/gravel).

Table 7. Eel River suspended, bed and bedload particle size distribution metrics[a]

		Suspended Sediment[b]				Bed[c]	Bedload[d]
Metric[e]	Unit	0 - 200 (m^3s^{-1})	200 - 2000 (m^3s^{-1})	2000 - 10000 (m^3s^{-1})	All Samples	All Samples	All Samples
Samples	n	5	117	58	180	7	6
Unimodal	n	1	1	0	2	2	2
Bimodal	n	1	23	20	44	4	3
Modality > 2	n	3	93	38	134	1	1
1° Mode mean	µm	3	66.66	22.84	50.77	12134	2813
1° Mode (s)	µm	0	143.82	56.71	122.11	11844	4616
2° Mode mean	µm	14.88	119.29	86.43	106.24	10650	20563
2° Mode (s)	µm	5.75	167.69	76.62	143.49	20907	32719
D_{10} mean	µm	2.40	2.80	2.74	2.77	287	432
D_{10} (s)	µm	0.12	0.42	0.18	0.36	162	283
D_{50} mean	µm	9.13	34.59	28.15	31.80	6352	2177
D_{50} (s)	µm	5.81	28.37	15.27	24.91	5759	2820
D_{90} mean	µm	113.44	308.67	197.31	267.36	18622	10114
D_{90} (s)	µm	100.25	149.67	0.00	136.74	17380	7904
Sorting mean	φ	1.88	2.45	2.26	2.37	2.12	2.21
Sorting (s)	φ	0.54	0.29	0.10	0.28	0.41	0.25
Skewness mean	φ	-0.91	-0.08	-0.03	-0.09	0.98	1.29
Skewness (s)	φ	1.80	0.30	0.23	0.32	1.07	0.69
Kurtosis (mean)	φ	3.25	1.79	1.83	1.85	5.29	7.57
Kurtosis (*s*)	φ	7.33	0.25	0.16	0.41	3.57	1.90
% Fines[f] mean	%	86.20	63.79	68.24	65.85	1.57	-
% Fines[f] (s)	%	16.72	11.00	6.96	11.09	2.64	-
% Clay mean	%	53.80	31.70	30.31	31.87	-	-
% Clay (s)	%	16.30	8.28	5.40	8.59	-	-
% Silt mean	%	32.40	32.09	37.93	33.98	-	-
% Silt (s)	%	3.71	7.24	4.40	7.01	-	-
% Sand mean	%	13.80	36.21	31.76	34.15	49.00	58.50
% Sand (s)	%	10.38	11.33	8.30	11.13	35.15	27.16
% Gravel mean	%	0	0	0	0	49.43	41.50
% Gravel (s)	%	-	-	-	-	36.95	27.16

[a]All samples collected and measured by the U.S. Geological Survey.

[b]Suspended sediment is further subdivided into populations based on discharge range.

[c]Bed samples were not processes for clay and silt classes, only the agregate class 'Fines.'

[d]No characterization of fines was performed on Bedload samples.

[e]All mean values are arithmetic. (s) indicates sample standard deviation. Sorting, skewness and kurtosis computed through the logarithmic method of moments.

[f]Fines includes the clay and silt classes.

Table 8. Comparisons of Eel River sediment mean particle size distribution characteristics[a].

Suspended sediment samples by discharge range.

Discharge ranges[b]			1° Mode	Sorting	Skewness	Kurtosis	D_{10}	D_{50}	D_{90}	% Clay	% Silt	% Sand
(Q < 200)	vs.	(Q > 200)	***	Eq.	*	Eq.	***	***	*	*	Eq.	**
(200 > Q > 2000)	vs.	(Q > 2000)	**	***	Eq.	Eq.	Eq.	*	***	Eq.	***	**

[a]Results for one sided T-tests listed as follows: (Eq.) indicates the H_0 of equivalent means was not rejected (P-value > 0.05), (*) for P-values < 0.05, (**) for P-values < 0.01, (***) for P-values < 0.001.

[b]Discharge ranges are reported in units of m^3s^{-1}.

Figure Captions

Figure 1. Generic model of abandoned channel fill sequence progression (based on Toonen *et al.* (2012)).

Figure 2. The lower Eel River Estuary study region (image date 6/27/2009). Fluvial flow direction is generally right to left, with the Eel River mouth to the Pacific Ocean visible in the upper left corner. The main northern Eel River channel system (the RSC complex) proceeds from Node 1 to Node 4. The Central Channel currently is the primary conveyance, while Ropers Slough is a tidal slough that receives high flows during the wet season. The star located toward the south east end of Ropers Slough indicates the location of the EDRS cores.

Figure 3. Aerial photo sequence of the Ropers Slough and Central Channel region in 1940, 1956, 1973, 2009. Ropers Slough is in the upper right portion of the frame and the Central Channel occupies center frame. The EDRS coring location is indicated by a yellow asterisk in each frame. All images are in the same scale and represent the same spatial extent.

Figure 4. Ropers Slough channel area diagrams for the (A) first (1948 – 1965) and (B) second (1974 to present) abandonment sequences. Both frames display the same scale and spatial extent.

Figure 5. Study region channel measurements. (a) Cutoff ratio of main to abandoned channel length. (b) Mean channel width of the study region channel reaches. (c) Ropers Slough channel width adjustment over the two abandonment periods, with channel width values normalized to average channel width in the most recent aerial photograph before abandonment. Channel

widths in all cases refer to active channel width defined by vegetated channel banks. Error ranges in temporal domain were only applied to measurements from image mosaics, which were collected in the summer of the given year, but without exact associated dates.

Figure 6. Distance of the tidal inlet to the coring site EDRS measured along the approximate thalweg of the intervening channel.

Figure 7. Stratigraphic and sedimentological results for the EDRS cores with ^{14}C chronology. See text for in depth descriptions.

Figure 8. Stratigraphy with carbon, nitrogen and ^{14}C chronology results. See text for in depth descriptions.

Figure 9. Eel River (A) suspended, (B) bed, and (C) bedload particle size distribution diagrams. All samples collected by the USGS at the Scotia gauge (#11477000) (USGS NWIS, 2014).

Figure 10. Log-linear concentration – discharge rating curves of Eel River suspended sediment by (A) texture class, and (B) the sand size classes of 'very fine' (62.5 to 125 µm) and 'fine' (125 to 250 µm).

Figure 11. Tanner (1991) domains of particle size distribution suite statistics for EDRS stratigraphic units and Eel River suspended, bed and bedload sediments. All figures are plotted in ϕ units, which increase in value with finer particle size.

Figure 12. Comparison of abandon channel fill stratigraphy with the number of years and hydrologic characteristics of the time period of deposition for Zones 1 and 4.

Figure 13. Zone 1 and Zone 4 stratigraphic unit characteristics and the estimated peak annual instantaneous discharge (Q_i) values for the Eel River Estuary during the period of deposition.

Figure 14. Selected EDRS sediment compositions in the context of Eel River suspended sediment and primary producers of organic material. The range and domain of Eel River suspended sediment values as per Goñi *et al.* (2013). Primary producer ranges in (B) are for fresh water phytoplankton (FW Phyto.), marine phytoplankton (Marine Phyto), and C_3 and C_4 vascular plants.

Figure 15. New conceptual model of abandoned channel fill progression incorporating alternating tidal/fluvial deposition.

Figure 16. Conceptual model for abandonment/reoccupation cycles in mixed fluvial/tidal estuarine channels.

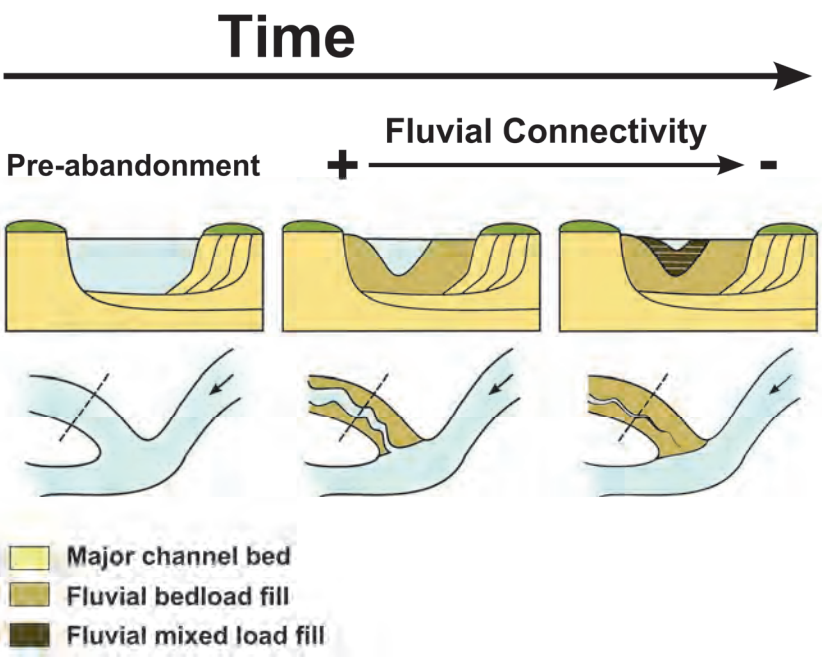
Time
Fluvial Connectivity
Pre-abandonment
+
-
Major channel bed
Fluvial bedload fill
Fluvial mixed load fill

Figure 1.

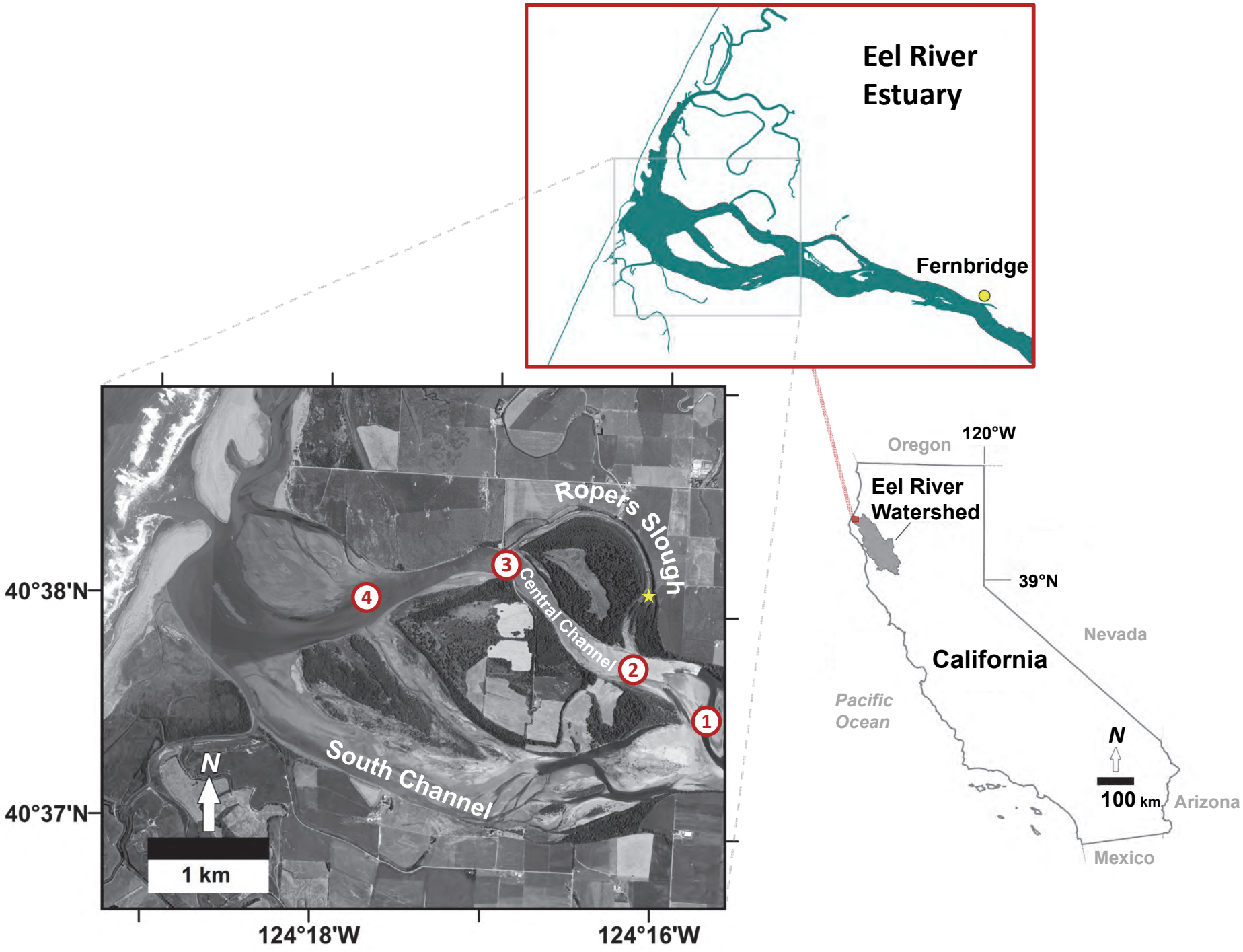
Eel River
Estuary
Fernbridge
Ropers Slough
Central Channel
South Channel
1
2
3
4
N
1 km
40°38'N
40°37'N
124°18'W
124°16'W
120°W
Oregon
Eel River
Watershed
39°N
Nevada
California
Pacific
Ocean
N
100 km
Arizona
Mexico

Figure 2.

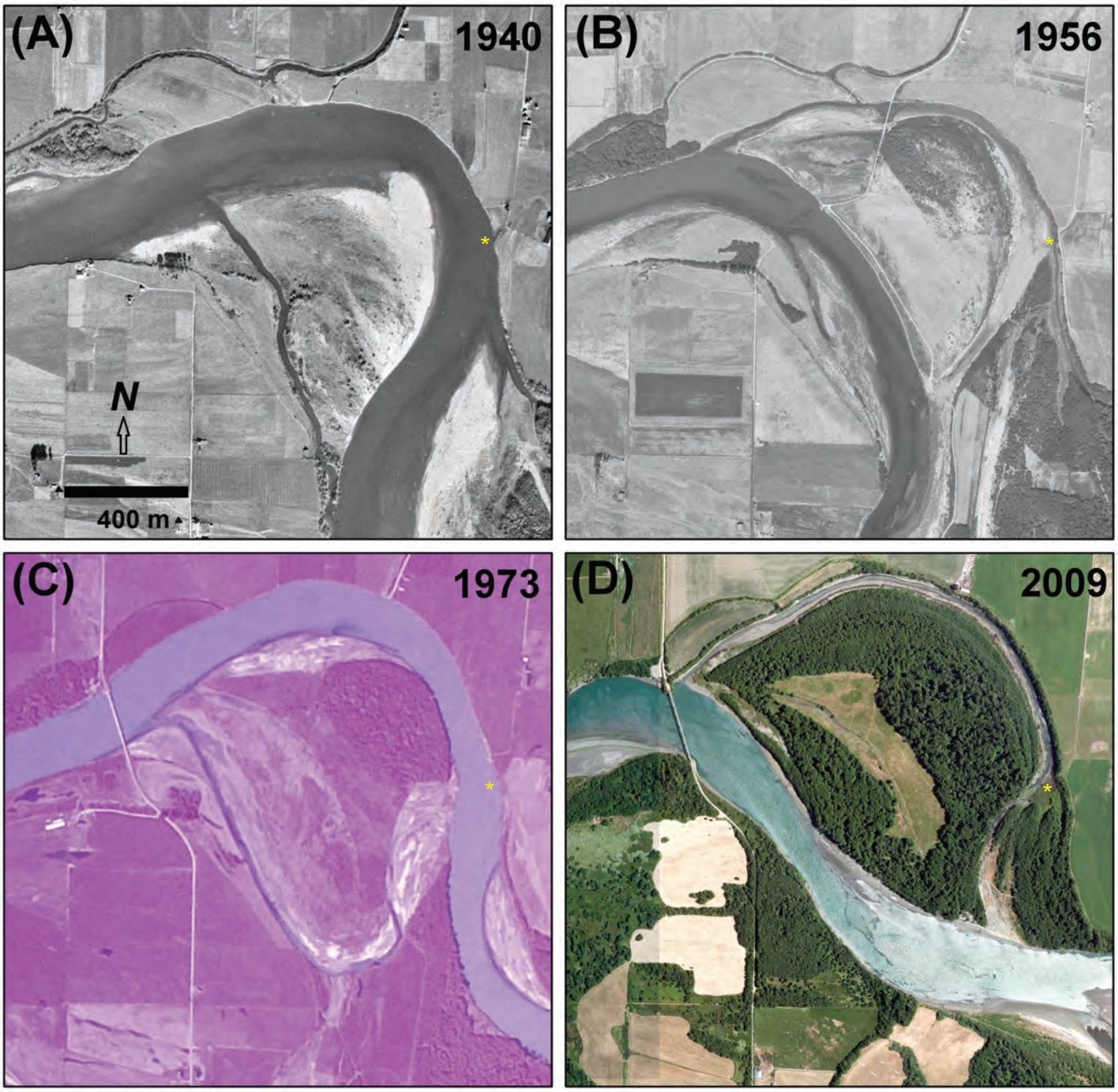

Figure 3.

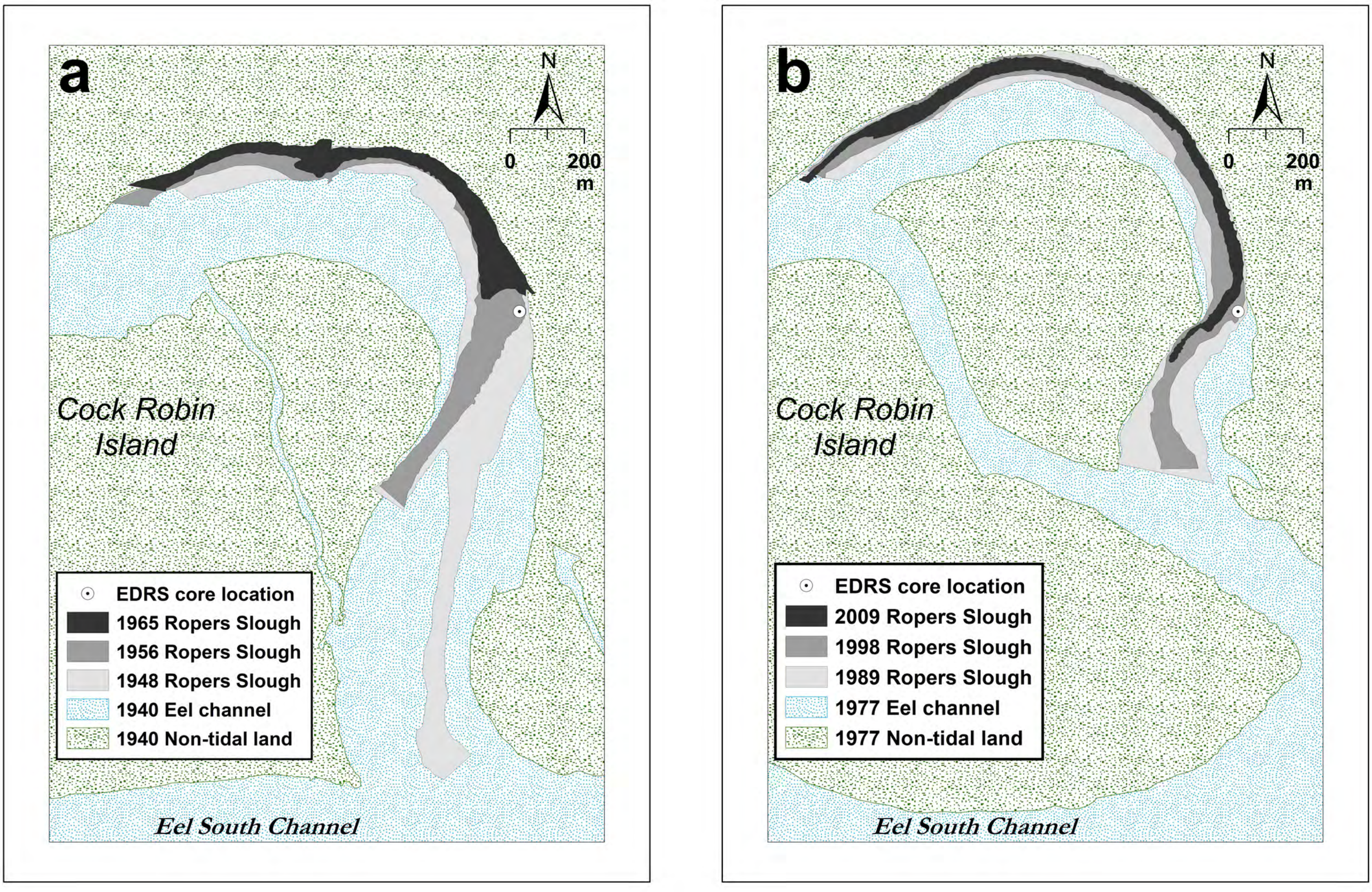
a
N
0
200
m
Cock Robin
Island
EDRS core location
1965 Ropers Slough
1956 Ropers Slough
1948 Ropers Slough
1940 Eel channel
1940 Non-tidal land
Eel South Channel
b
N
0
200
m
Cock Robin
Island
EDRS core location
2009 Ropers Slough
1998 Ropers Slough
1989 Ropers Slough
1977 Eel channel
1977 Non-tidal land
Eel South Channel

Figure 4.

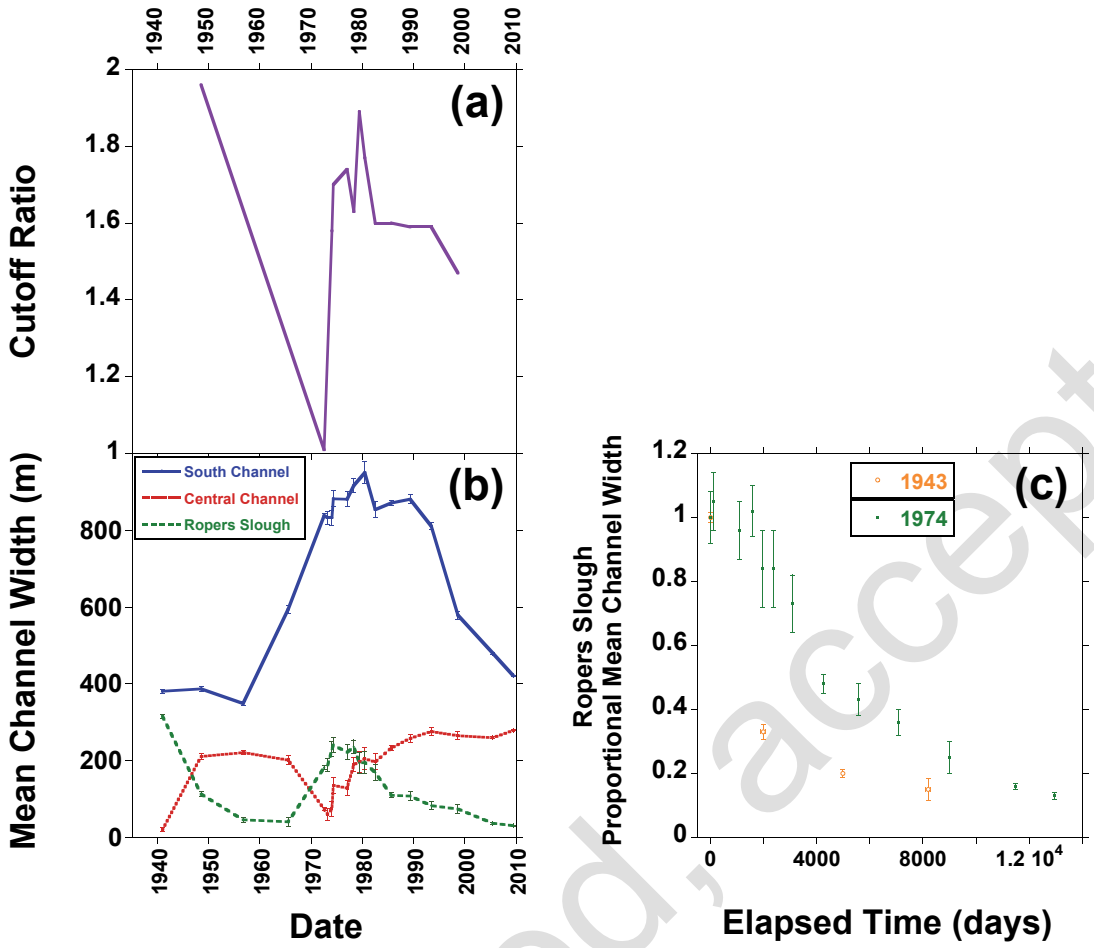

Figure 5.

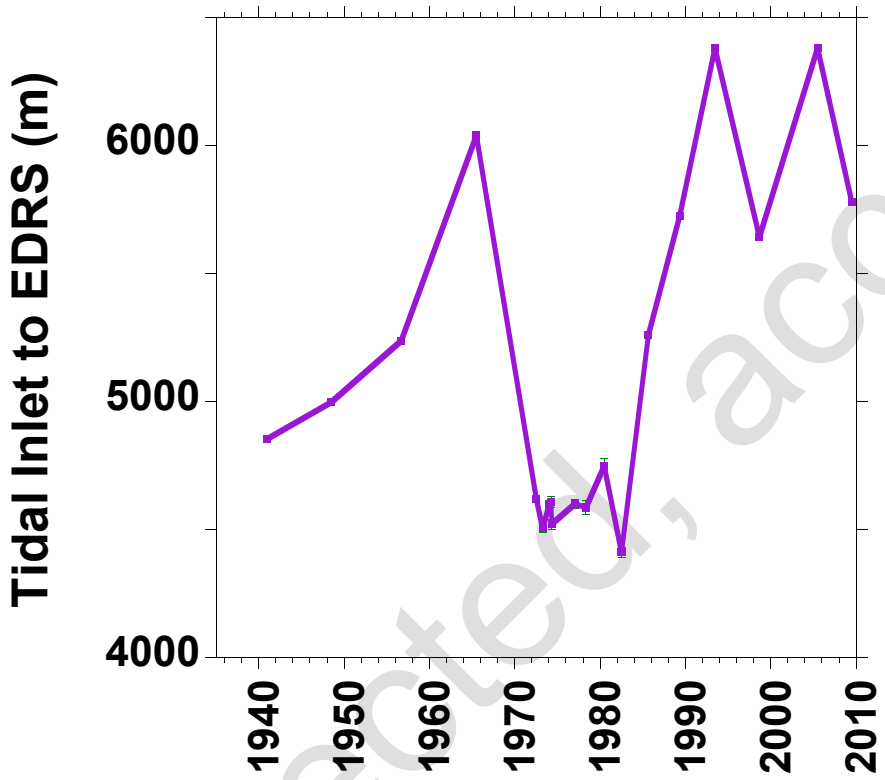

Figure 6.

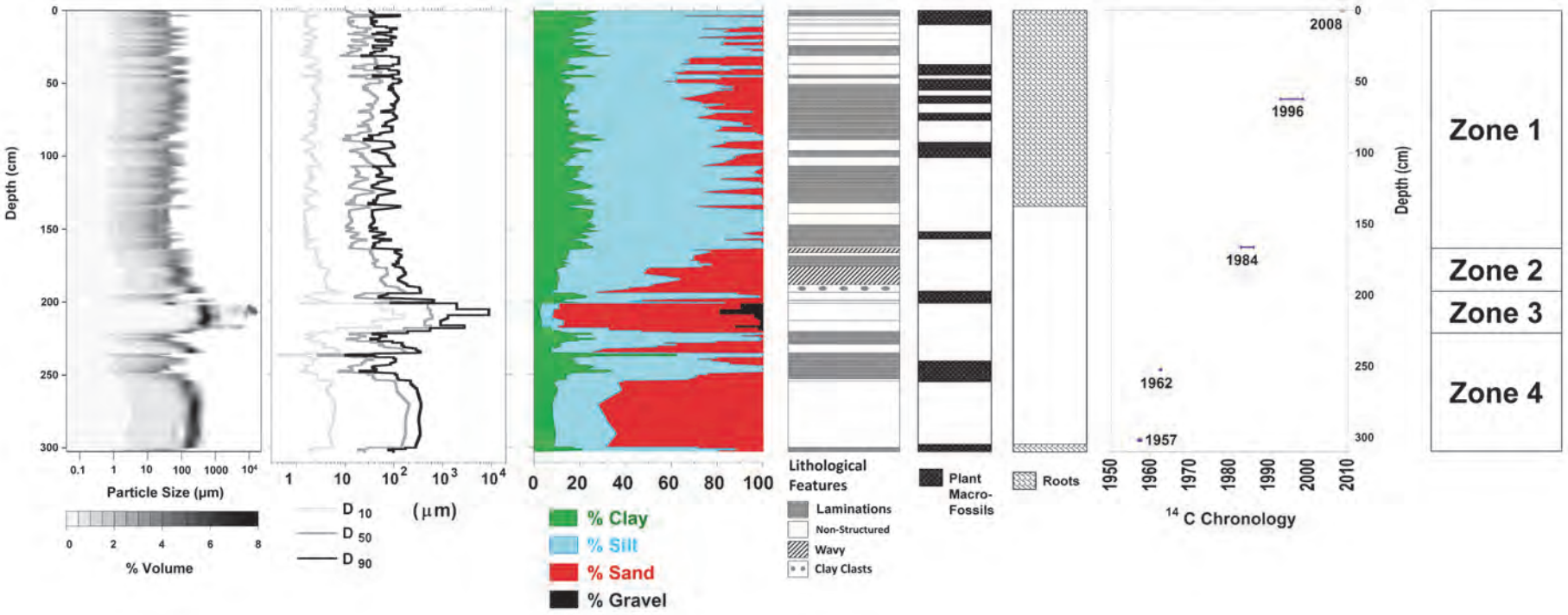

Figure 7.

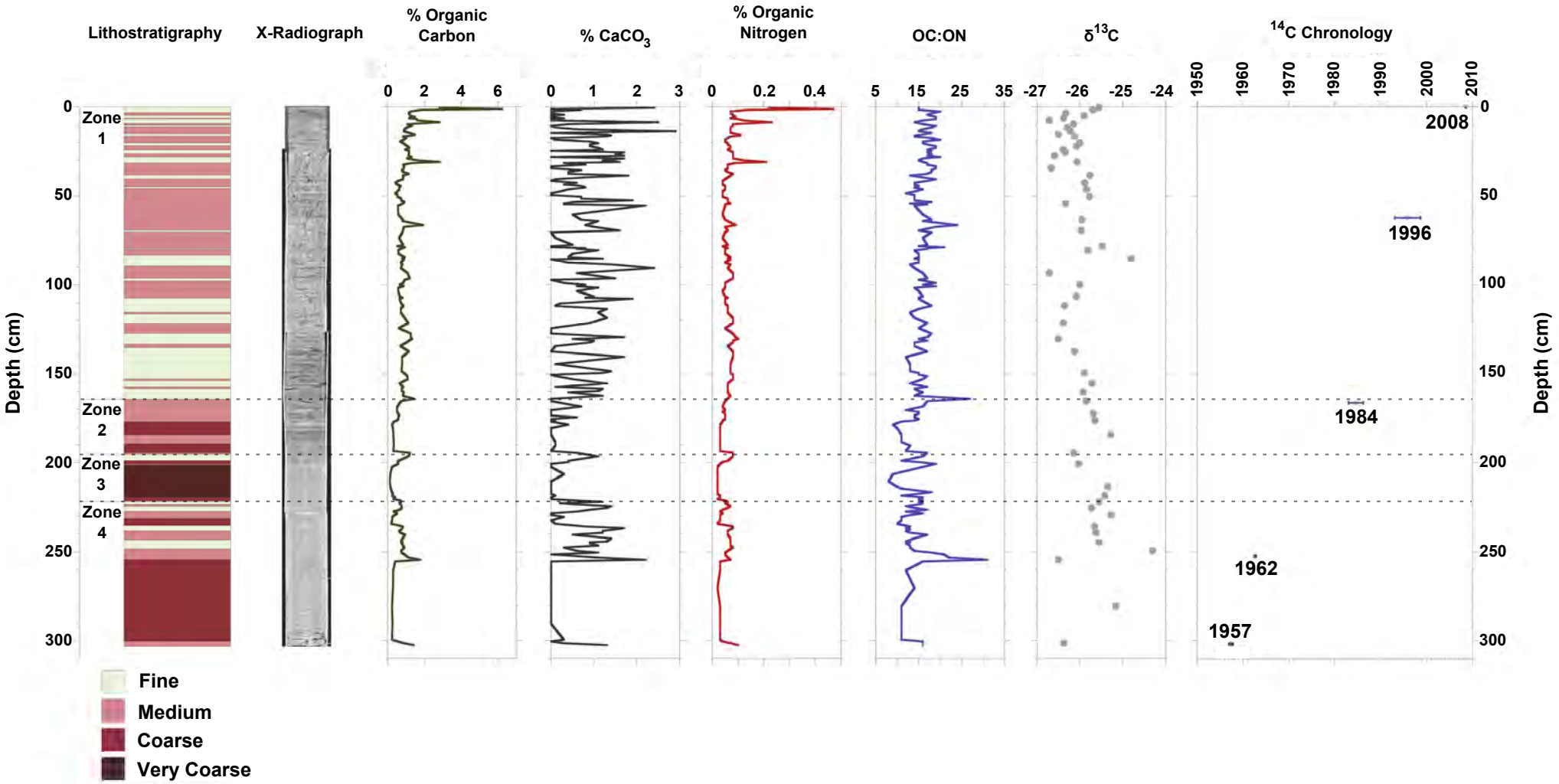
Lithostratigraphy
X-Radiograph
% Organic Carbon
% CaCO3
% Organic Nitrogen
OC:ON
δ13C
14C Chronology
Depth (cm)
Zone 1
Zone 2
Zone 3
Zone 4
2008
1996
1984
1962
1957
Fine
Medium
Coarse
Very Coarse

Figure 8.

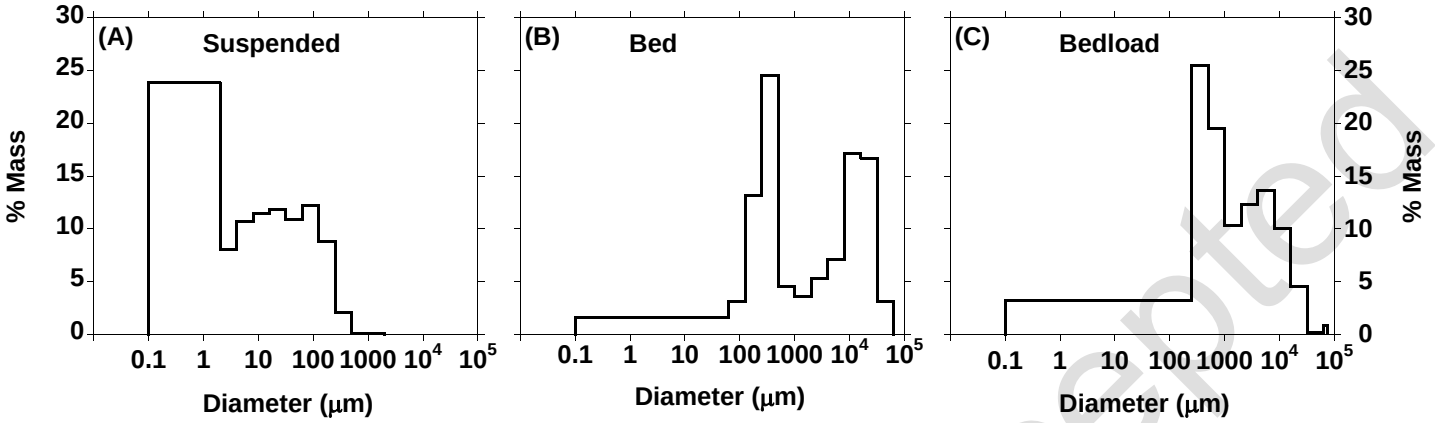

Figure 9.

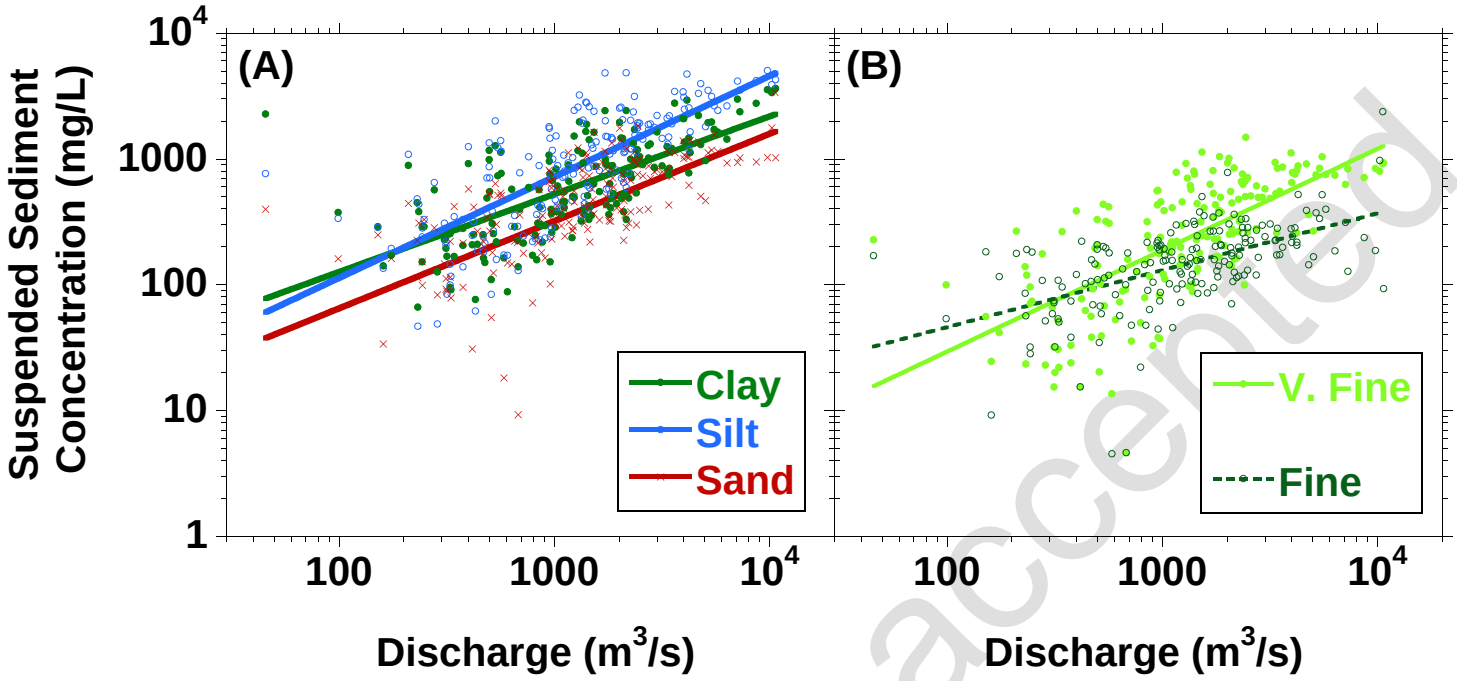

Figure 10.

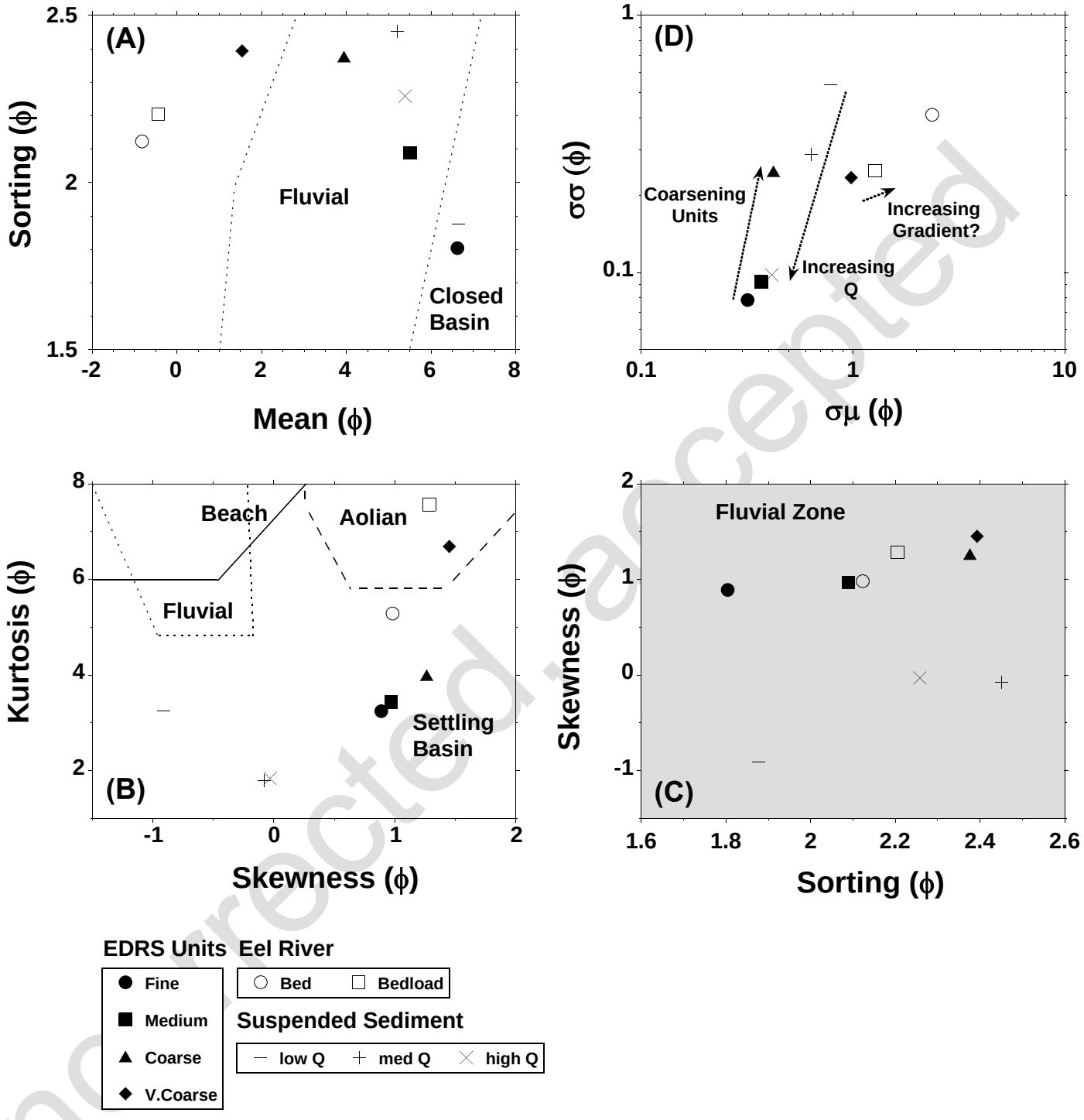

Figure 11.

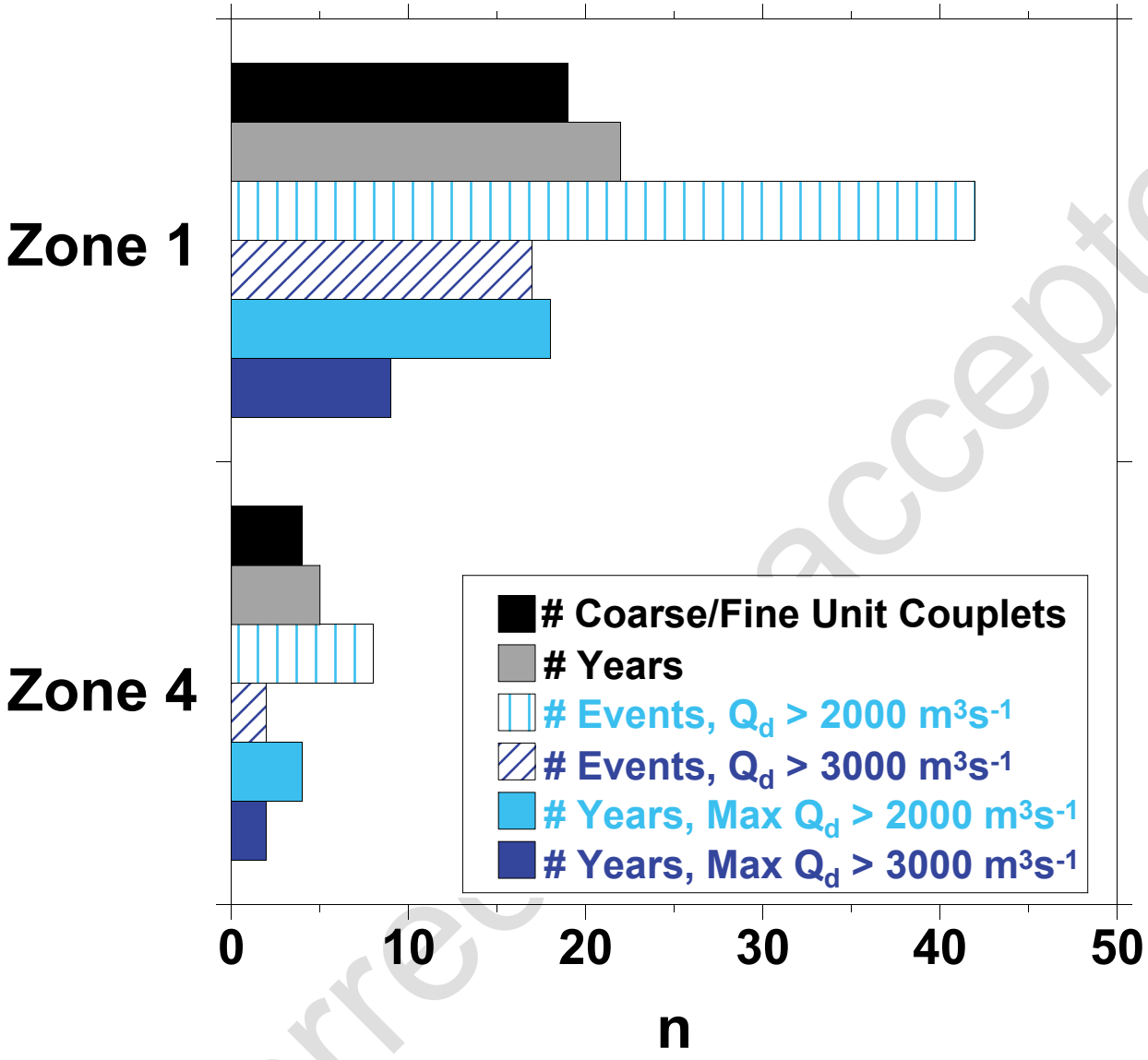

Figure 12.

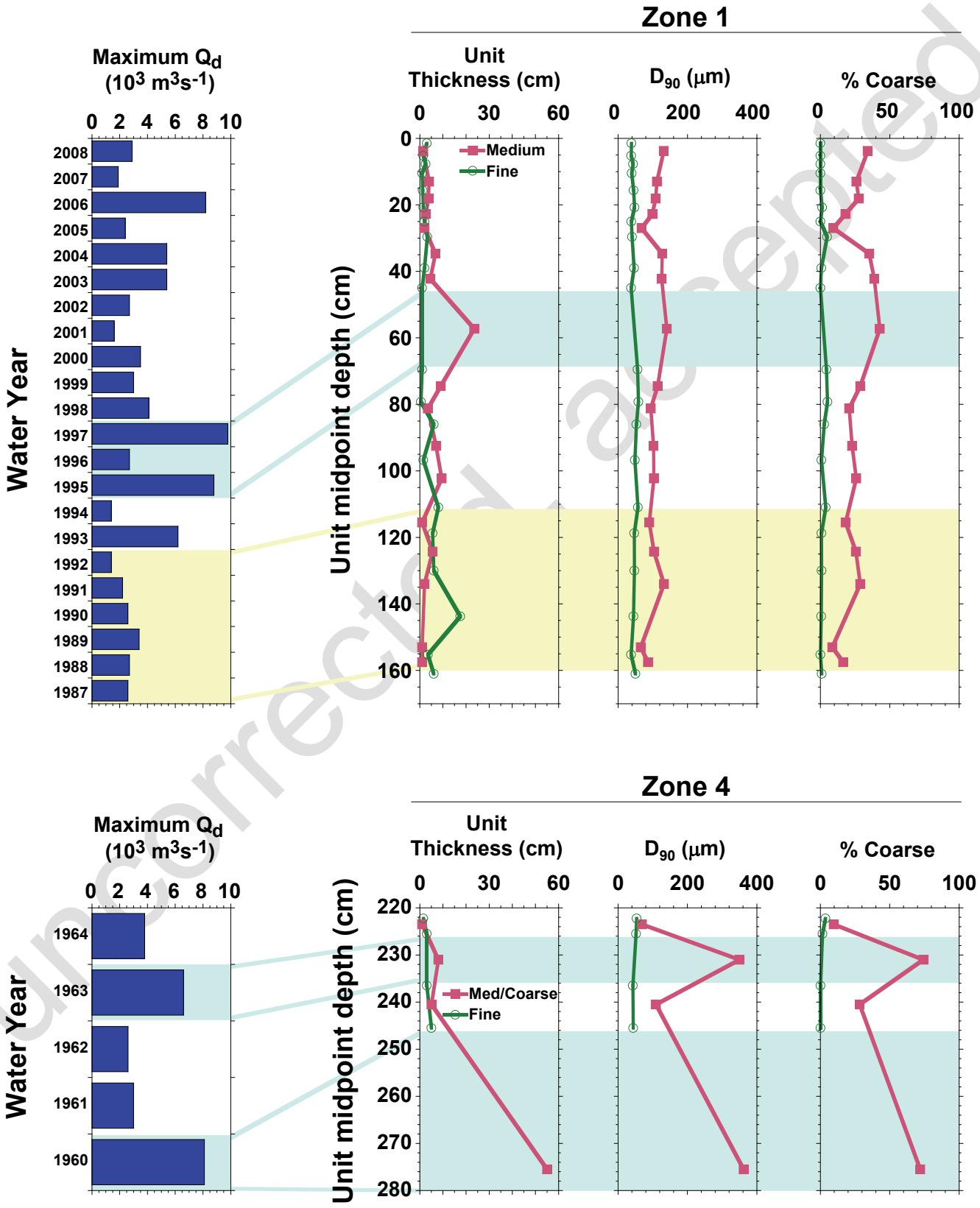

Figure 13.

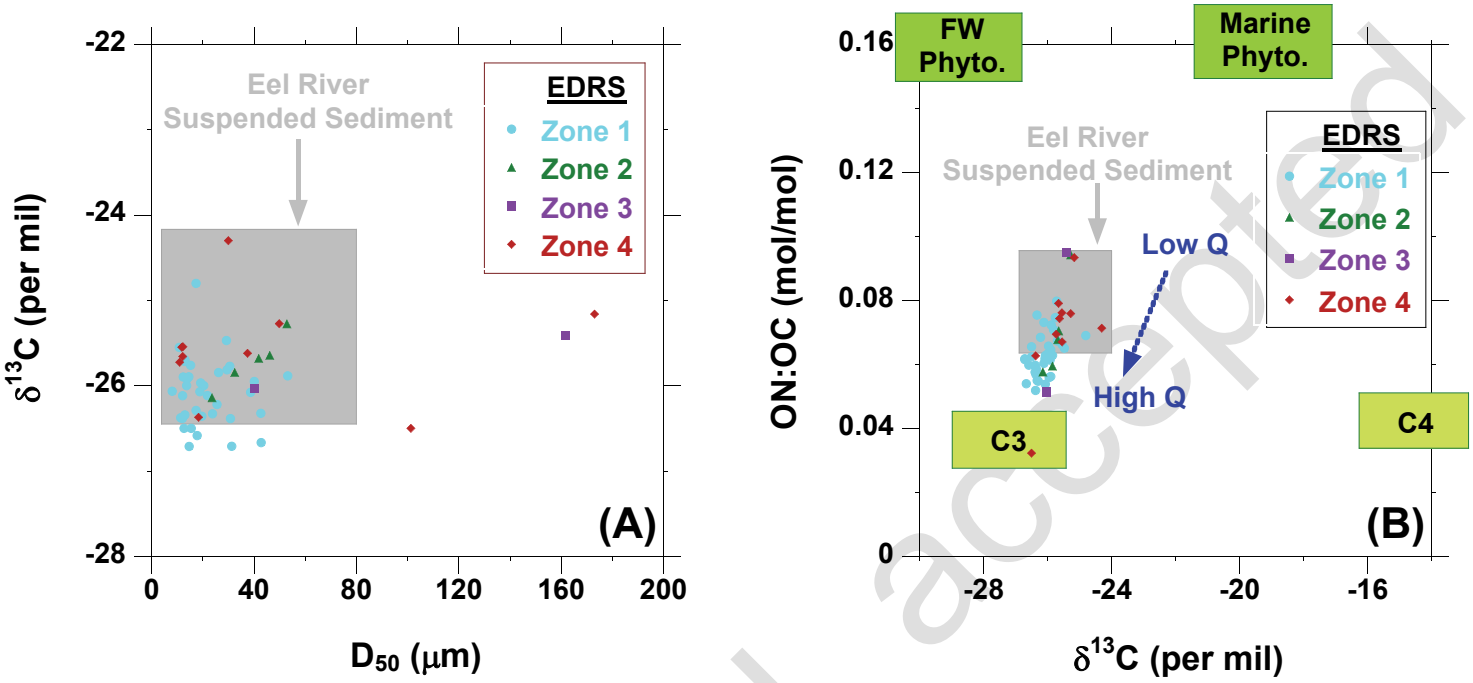

Figure 14.

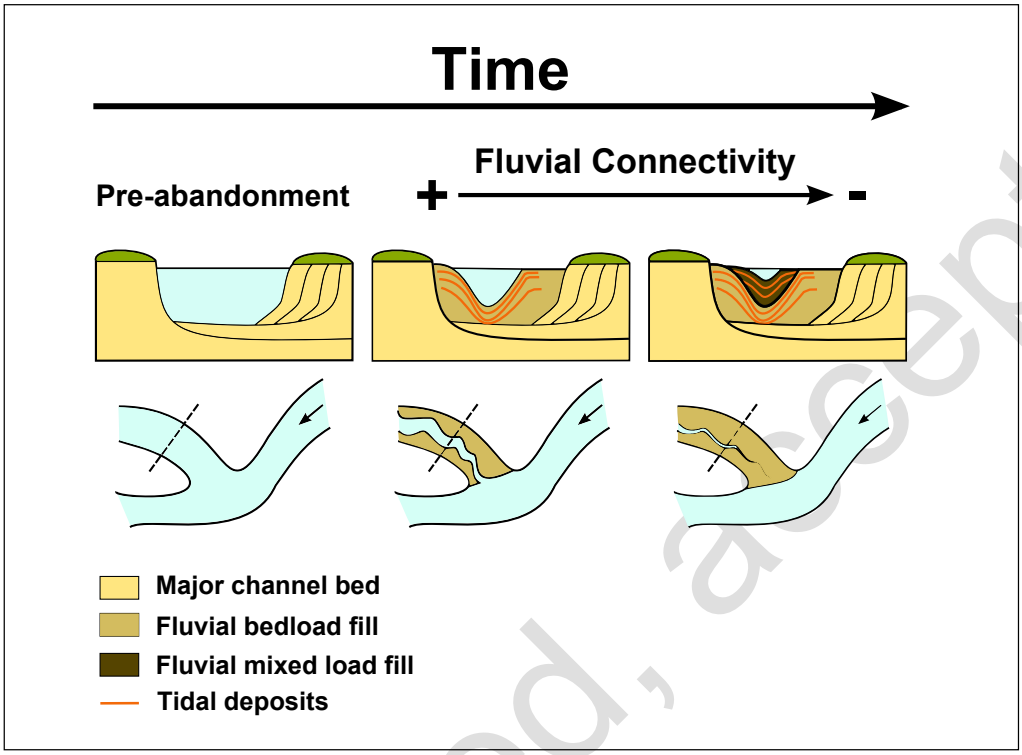

Figure 15.

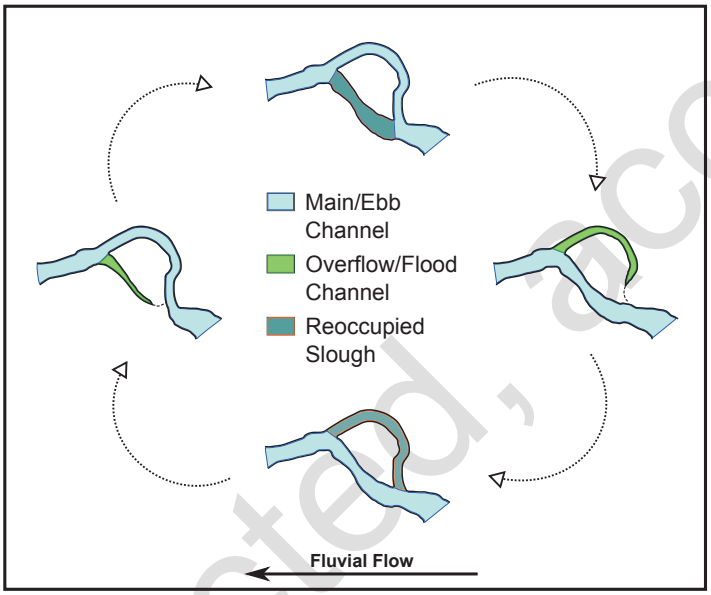

Figure 16.

Appendix I. Particle size distribution characteristics of horizons by stratigraphic zone

Of the 46 measured fine horizons, 37 were present in Zone 1, and 9 in Zone 4 (Table 4). Fine horizons were poorly sorted, mesokurtic, and fine skewed, displaying single or bimodal peaks in the medium to very coarse silt range (11–38 μm) and a characteristic clay shoulder around 2–4 μm (App. Table 1, App. Fig. 1). Clay/Silt ratios were generally 1:3.

Sandy horizons displayed a greater range of particle size distribution characteristics than fine horizons (Table 4, Fig. 7). In general, sandy horizons were very poorly sorted, mesokurtic to very leptokurtic, fine skewed, and unimodal, with a small proportion of bimodal and poly-modal horizons found mostly in Zones 3 and 4. Primary modes in Zones 1, 2 and 4 were generally in the coarse silt to very fine sand range (31–125 μm). The few secondary modalities in these zones were generally finer, plotting in the coarse to very coarse silt range. In contrast, the majority of Zone 3 horizons were fine skewed, meso to leptokurtic, and bimodal or poly-modal mixes of sand and gravel. Zone 3 primary modes ranged from fine to medium sand (125–500 μm), while secondary modes were generally coarser, plotting in the very coarse sand to medium gravel range ($1{\cdot}10^3$–$1.6{\cdot}10^5$ μm). High variability in texture class composition also belied the range of sediments represented by this group, as horizons varied between clayey silts, with trace amounts of sand, to sand and gravel mixes with very low (<10%) fines (App. Fig. 1).

Appendix II. Facies units

Horizons were aggregated into facies units, defined as contiguous horizons with specific grain characteristics. First, horizon types were refined, as highly variable sandy horizon particle size characteristics within and between zones suggested that further delimitation was necessary. A histogram of sandy horizons by % coarse revealed that three disparate populations of sandy samples were likely: samples with trace (< 7%), moderate (7–50 %) and high (> 50%) coarse content with and without gravel (App. Fig. 2). All sandy populations significantly differed from each other in terms of all mean particle sized distribution descriptors, with the exception of some comparisons to samples with gravel, which were obscured by the high variance of most particle size distribution metrics for these samples (App. Table 2). Thus, horizons were grouped into four characteristic facies unit types: (i) Fine (0–7 % sand), (ii) Medium (7–50 % sand), (iii) Coarse (> 50% sand, no gravel), and (iv) Very Coarse (gravelly sand).

Appendix Table 1. EDRS particle size distribution metrics by horizon type and zone

		Fine Horizons[a]					Sandy Horizons[b]				
Metric[c]	Unit	Zone1	Zone2	Zone 3	Zone 4	All Zones	Zone1	Zone2	Zone 3	Zone 4	All Zones
Horizons	n	37	0	0	9	46	89	16	14	30	149
Unimodal	n	13	0	0	4	17	87	14	5	22	128
Bimodal	n	24	0	0	5	29	1	1	5	5	12
Modality > 2	n	0	0	0	0	0	1	1	4	3	9
1° Mode mean	µm	28.68	-	-	25.05	27.97	45.80	76.59	318.43	80.16	90.03
1° Mode (s)	µm	8.97	-	-	10.20	9.22	20.70	45.19	203.74	74.80	102.74
2° Mode mean	µm	23.65	-	-	20.86	23.17	36.63	16.42	1199	45.80	1106
2° Mode (s)	µm	7.71	-	-	12.95	8.60	7.20	0	5651	42.69	3788
Sorting mean	φ	1.77	-	-	1.75	1.76	2.00	2.15	2.40	2.14	2.08
Sorting (s)	φ	0.04	-	-	0.08	0.05	0.12	0.12	0.31	0.19	0.20
Skewness mean	φ	0.86	-	-	0.80	0.85	0.95	1.13	1.19	1.05	1.01
Skewness (s)	φ	0.05	-	-	0.08	0.06	0.11	0.24	0.53	0.28	0.25
Kurtosis (mean)	φ	3.18	-	-	3.03	3.15	3.37	3.84	4.78	3.60	3.60
Kurtosis (*s*)	φ	0.11	-	-	0.17	0.14	0.24	0.64	2.34	0.59	0.89
% Clay mean	%	25.42	-	-	31.42	26.60	17.20	12.41	9.72	14.12	15.36
% Clay (s)	%	2.06	-	-	12.09	5.93	2.96	1.93	0.53	4.87	4.55
% Silt mean	%	74.58	-	-	68.58	73.40	67.02	51.02	31.53	51.55	58.85
% Silt (s)	%	2.06	-	-	12.09	5.93	9.26	10.04	24.52	20.40	17.99
% Coarse mean	%	0	-	-	0	0	15.78	36.57	58.74	34.34	25.79
% Coarse (s)	%	0	-	-	0	0	11.88	11.62	28.09	24.92	22.27

[a]Fine horizons are defined as those that were composed only of clay and silt size classes. [b]Sandy horizons are those that contain andy amount of sand sized or coarser inorganic material. [c]All mean values are arithmetic. (*s*) indicates sample standard deviation. Sorting, skewness and kurtosis computed through the logarithmic method of moments.

Appendix Table 2. Comparison of particle size distribution characteristics by facies unit[a].

Facies Unit[b]			1° Mode	Sorting	Skewness	Kurtosis	D_{10}	D_{50}	D_{90}	% Clay	% Silt	% Coarse[c]
Fine	vs.	Medium	***	***	*	*	***	***	***	***	***	***
Fine	vs.	Coarse	***	***	***	**	**	***	***	***	***	***
Fine	vs.	Very Coarse	**	**	Eq	*	*	**	Eq.	***	***	***
Medium	vs.	Coarse	***	***	***	**	*	***	***	***	***	***
Medium	vs.	Very Coarse	**	*	Eq	*	*	**	Eq.	***	***	***
Coarse	vs.	Very Coarse	**	Eq.	Eq	Eq.	*	**	Eq.	**	**	**

[a]Results for one sided T-tests listed as follows: (Eq.) indicates the H_0 of equivalent means was not rejected (P-value > 0.05), (*) for P-values < 0.05, (**) for P-values < 0.01, (***) for P-values < 0.001.

[b]Facies units refer to all horizons with the indicated ranges of % coarse: Fine = (0-7%); Medium = (7-50%); Coarse = (>50% no gravel); Very Coarse = (>50% w/gravel).

[c]The descriptor % coarse is the sum of % sand and % gravel.

Appendix Figure 1. Coarse (sand + gravel) content histogram.

Appendix Figure 2. Characteristic particle size distributions for horizon types by zone and general coarse (sand + gravel) content. Figures correspond to the following EDRS depths (cm): (A) 24-24.5, (B) 127-127.5, (C) 27-28, (D) 82-83, (E) 48-49 43%(F) 174-175, (G) 193-194, (H) 196-197, (I) 220-221, (J) 205-209, (K) 236-237, (L) 237.25-238, (M) 301-302, (N) 239-240, (O) 270-271.

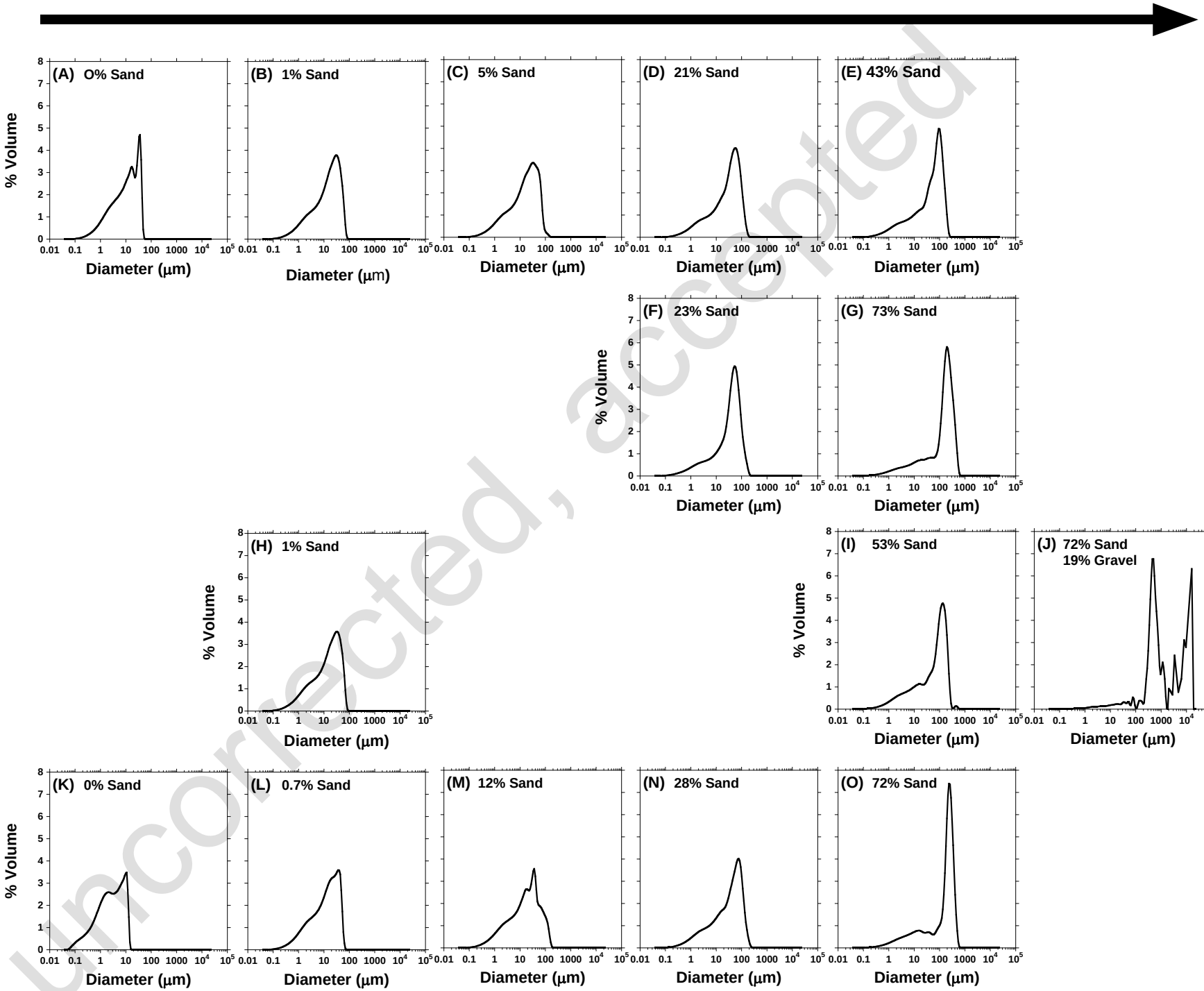

Appendix Figure 1.

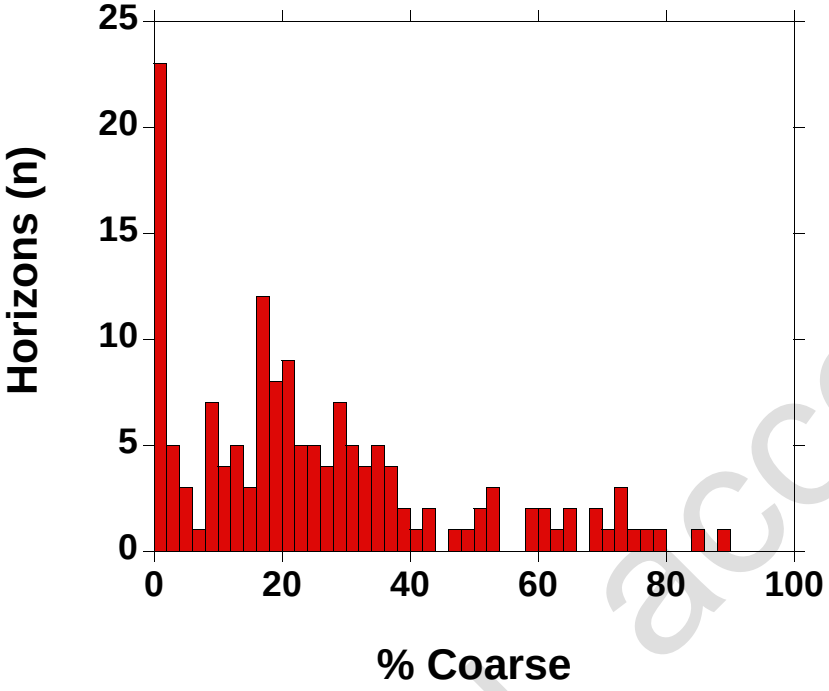

Appendix Figure 2.